2001-12

Experimental determination of paraxial ray transfer matrices and cardinal points of complex optical systems by means of finite conjugate imaging

Blackwell, Jerry S.

Monterey, California. Naval Postgraduate School

NAVAL POSTGRADUATE SCHOOL
Monterey, California

THESIS

EXPERIMENTAL DETERMINATION OF PARAXIAL RAY TRANSFER MATRICES AND CARDINAL POINTS OF COMPLEX OPTICAL SYSTEMS BY MEANS OF FINITE CONJUGATE IMAGING

by

Jerry S. Blackwell

December 2001

Thesis Advisor: D. Scott Davis
Second Reader: Richard Harkins

Approved for public release; distribution is unlimited.

THIS PAGE INTENTIONALLY LEFT BLANK

REPORT DOCUMENTATION PAGE	*Form Approved OMB No. 0704-0188*

1. AGENCY USE ONLY ***(Leave blank)***	**2. REPORT DATE** December 2001	**3. REPORT TYPE AND DATES COVERED** Master's Thesis

4. TITLE AND SUBTITLE: **Experimental Determination of Paraxial Ray Transfer Matrices and Cardinal Points of Complex Optical Systems by Means of Finite Conjugate Imaging**

5. FUNDING NUMBERS

6. AUTHOR(S) Blackwell, Jerry S.

7. PERFORMING ORGANIZATION NAME(S) AND ADDRESS(ES)
Naval Postgraduate School
Monterey, CA 93943-5000

8. PERFORMING ORGANIZATION REPORT NUMBER

9. SPONSORING / MONITORING AGENCY NAME(S) AND ADDRESS(ES)
N/A

10. SPONSORING / MONITORING AGENCY REPORT NUMBER

11. SUPPLEMENTARY NOTES The views expressed in this thesis are those of the author and do not reflect the official policy or position of the Department of Defense or the U.S. Government.

12a. DISTRIBUTION / AVAILABILITY STATEMENT
Approved for public release; distribution is unlimited.

12b. DISTRIBUTION CODE

13. ABSTRACT ***(maximum 200 words)***

The Lineate Imaging Near-ultraviolet Spectrometer (LINUS) uses three complex lens systems to focus an image from distances on the order of several kilometers onto the image intensifier of an ultraviolet camera. These images can then be analyzed to characterize the atmospheric distribution and concentration of sulfur dioxide (SO_2). The lenses purchased for LINUS were corrected for spherical aberrations but due to the lack of detailed knowledge about the lenses their chromatic aberrations could not be readily predicted. The project presented in this thesis was performed with the goal of experimentally quantifying the chromatic aberrations of each of LINUS's lens systems.

The matrix method of representing paraxial optical systems was used to determine relationships between object and image distances for different lens systems. These relationships were manipulated to give equations for the matrix elements of the lens system in terms of readily measurable parameters. Once the matrix elements are known, all of the cardinal points can be readily predicted. This method will, in theory, quantify the chromatic aberrations of each lens system. The method was validated with simulations and measurements taken on a lens of known focal length. Finally, the LINUS lens systems were characterized at 220, 300, 334, and 370 nm.

14. SUBJECT TERMS ULTRAVIOLET SPECTROSCOPY, MATRIX METHOD, COMPLEX LENS SYSTEMS

15. NUMBER OF PAGES

16. PRICE CODE

17. SECURITY CLASSIFICATION OF REPORT	**18. SECURITY CLASSIFICATION OF THIS PAGE**	**19. SECURITY CLASSIFICATION OF ABSTRACT**	**20. LIMITATION OF ABSTRACT**
Unclassified	Unclassified	Unclassified	UL

THIS PAGE INTENTIONALLY LEFT BLANK

Approved for public release; distribution is unlimited.

EXPERIMENTAL DETERMINATION OF PARAXIAL RAY TRANSFER MATRICES AND CARDINAL POINTS OF COMPLEX OPTICAL SYSTEMS BY MEANS OF FINITE CONJUGATE IMAGING

Jerry S. Blackwell
Lieutenant, United States Navy
B.S., University of Texas at Austin, 1994

Submitted in partial fulfillment of the
requirements for the degree of

MASTER OF SCIENCE IN APPLIED PHYSICS

from the

NAVAL POSTGRADUATE SCHOOL
December 2001

Author: Jerry S. Blackwell

Approved by: Scott Davis, Thesis Advisor

Richard Harkins, Second Reader

William Maier, Chairman, Department of Physics

THIS PAGE INTENTIONALLY LEFT BLANK

ABSTRACT

The Lineate Imaging Near-ultraviolet Spectrometer (LINUS) uses three complex lens systems to focus an image from distances on the order of several kilometers onto the image intensifier of an ultraviolet camera. These images can then be analyzed to characterize the atmospheric distribution and concentration of sulfur dioxide (SO_2). The lenses purchased for LINUS were corrected for spherical aberrations but due to the lack of detailed knowledge about the lenses their chromatic aberrations could not be readily predicted. The project presented in this thesis was performed with the goal of experimentally quantifying the chromatic aberrations of each of LINUS's lens systems.

The matrix method of representing paraxial optical systems was used to determine relationships between object and image distances for different lens systems. These relationships were manipulated to give equations for the matrix elements of the lens system in terms of readily measurable parameters. Once the matrix elements are known, all of the cardinal points can be readily predicted. This method will, in theory, quantify the chromatic aberrations of each lens system. The method was validated with simulations and measurements taken on a lens of known focal length. Finally, the LINUS lens systems were characterized at 220, 300, 334, and 370 nm.

THIS PAGE INTENTIONALLY LEFT BLANK

TABLE OF CONTENTS

LIST OF FIGURES

THIS PAGE INTENTIONALLY LEFT BLANK

LIST OF TABLES

THIS PAGE INTENTIONALLY LEFT BLANK

ACKNOWLEDGMENTS

The author would like to thank Professors Scott Davis and Richard Harkins for their guidance and patience during this process. Special thanks are also given to my wife and children, Teresa, Ryan, Seth, and Sara, for their patience and understanding during the final portions of research and writing. Finally, the author would like to thank his Lord and Savior, Jesus Christ, for blessing him with the ability to perform this research.

THIS PAGE INTENTIONALLY LEFT BLANK

I. INTRODUCTION

A. MOTIVATION AND OBJECTIVES

Ultraviolet (UV) and near-ultraviolet spectroscopy research has been ongoing at the Naval Postgraduate School since 1990. The first such instrument developed here was the **M**iddle **U**ltraviolet **S**pec**T**rograph for **A**nalysis of **N**itrogen **G**ases (MUSTANG), a rocket-borne instrument intended to analyze emission line spectra in the earth's ionosphere. MUSTANG was later upgraded from a conventional spectrograph to an imaging spectrometer resulting in the **D**ual **U**se **U**ltra**V**iolet **I**maging **S**pectrometer (DUUVIS). DUUVIS was tested early in 1997. However, the images that it produced were not of acceptable quality, and a new instrument was needed. The next step toward hyperspectral imaging was taken with an entirely new instrument, the **N**PS **U**ltra**V**iolet **I**maging **S**pectrometer (NUVIS). NUVIS became operational in the fall of 1997 and was field-tested using chemical effluent plumes from industrial smokestacks. Results from this testing, analyzed by LT Stephen Marino, demonstrated the ability of the instrument to characterize sulfur dioxide (SO_2) distribution and concentration in industrial chemical plumes. LT Marino's work also revealed several limitations inherent in NUVIS's design [1]. One of the more severe limitations of NUVIS was its inability to observe any spectra other than that of SO_2. Rather than attempt to upgrade NUVIS, it was decided to build a new instrument capable of hyperspectral imaging across the entire 200-400nm ultraviolet spectral region. Thus, the design for LINUS, the **L**ineate **I**maging **N**ear-**U**ltraviolet **S**pectrometer was conceived. [1]

Traditionally, the unavailability of acceptable refractive materials with low UV absorption properties has required that UV instruments consist of reflective optics. However, LINUS' design is based on both reflective and refractive optics due to the recent development of low-absorption UV glass. This has permitted the design of an aplanatic instrument, one whose optics are corrected for several basic aberrations.

The research described in this thesis has focused on the characterization of the complex lens systems used in the LINUS instrument. Each lens system was characterized at several different wavelengths to ensure accurate operation at wavelengths other than that characteristic of SO_2. Several steps were taken in the solution of this particular problem. First, the method for determining the lens matrix for each lens system was developed. Next, a series of 'thought experiments' were conducted to verify the utility of the selected method. Once the method had been verified it was tested using a thin lens and visible light in the laboratory. Finally, data was taken and analyzed using the actual LINUS lens systems.

B. OUTLINE

This thesis is comprised of five chapters and two appendices. Chapter II contains a brief description of the ray transfer matrix method of characterizing optical systems and describes the method used to characterize simple lens systems. It also contains the results of the 'thought experiments' used to validate the method. Chapter III outlines and verifies the method, which can be used to analyze the characteristics of complex lens systems in a manner very similar to that used for simple lens systems in Chapter II. Chapter IV presents the measurement, analysis, and characterization of each LINUS lens system at selected wavelengths across the near-UV spectral region. Conclusions and recommendations for future work are discussed in Chapter V. The appendices contain both raw experimental data, and various Matlab programs written to perform the data analysis.

II. DETERMINATION OF MATRIX ELEMENTS FOR SIMPLE OPTICAL SYSTEMS

A. THE MATRIX METHOD

Approximately 25 years ago several innovative researchers developed a simple matrix-algebraic approach for the geometrical optical characterization of paraxial systems.[2] Due to its ease of use, this method was the one chosen as the basis for this thesis research. The basic concepts of this method are presented here as an aid to understanding how this method was employed in the determination of thin and complex lens system characteristics.

1. Paraxial Optics

Use of the matrix method hinges on the assumption that the optical system being analyzed is paraxial. The paraxial behavior regime applies whenever the angle between the system's optical axis and the ray of interest (α, in Fig. 1) is small. This allows use of the small angle approximations ($\sin(\alpha) \approx \alpha$, $\tan(\alpha) \approx \alpha$, and $\cos(\alpha) \approx 1$) when tracing the path of the ray through the optical system. A simple paraxial system is shown in Figure 1.

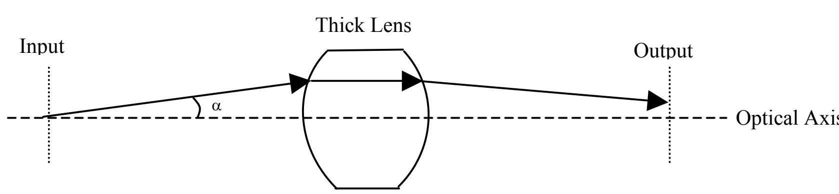

Figure 1. A simple paraxial optical system.

2. Matrix Representation of Geometrical Optics

Each of the three arrows seen above represents a translation of the light from one point in space to another. In each of the three regions, the ray follows a straight line-segment that makes a constant angle between the ray and the optical axis. At points where the ray meets a lens face or other discontinuity in refractive index, Snell's law dictates that the ray change its angle with respect to the optical axis. This constitutes a point operation.

First one must find a way to define any point in the ray's trajectory. The easiest way to accomplish this task is to use an angle and height format. Height of the ray (y) is measured from the optical axis. The first ray in Figure 1 has an origin, the input plane, and an ending point, the first face of the lens. The point of origin is written (α_1, y_1), and the ending point is, similarly (α_2, y_2). Assume that this ray has traveled a distance L, along the optical axis. The actual distance that this ray has translated is $L \cdot \cos(\alpha)$ but since a is so small the paraxial approximation applies and the distance translated is very closely approximated by L. Similarly, the ray has moved away from the optical axis by the amount, $L \cdot \tan(\alpha)$ which can be approximated as $L \cdot \alpha$. The following relationships can be determined simply by inspection of the ray in question.

$$\alpha_2 = \alpha_1, \text{ and}$$

$$y_2 = y_1 + \alpha_1 L.$$

These equations can be written in matrix form as follows:

$$\begin{bmatrix} y_2 \\ \alpha_2 \end{bmatrix} = M_1 \cdot \begin{bmatrix} y_1 \\ \alpha_1 \end{bmatrix} = \begin{bmatrix} 1 & L \\ 0 & 1 \end{bmatrix} \cdot \begin{bmatrix} y_1 \\ \alpha_1 \end{bmatrix}.$$

Before the ray undergoes its second translation the angle that it makes with the optical axis changes, or refracts, with no change in height. In this case y_2 is obviously equal to y_3. The change in angle is governed by Snell's law, which, in its paraxial form, gives the following relationship.

$$\alpha_3 = \left(\frac{1}{R}\right) \cdot \left(\frac{n}{n'} - 1\right) \cdot y_2 + \left(\frac{n}{n'}\right) \alpha_2 .$$

Where n and n' are the indices of refraction on the left and right sides of the interface and R is the radius of curvature of the interface. When combined with the fact that height stays constant for this point operation the equations can be written in the matrix form,

$$\begin{bmatrix} y_3 \\ \alpha_3 \end{bmatrix} = M_2 \cdot \begin{bmatrix} y_2 \\ \alpha_2 \end{bmatrix} = \begin{bmatrix} 1 & 0 \\ \frac{n - n'}{Rn} & \frac{n}{n'} \end{bmatrix} \cdot \begin{bmatrix} y_2 \\ \alpha_2 \end{bmatrix}. \text{[3, pp. 66-67]}$$

Any paraxial optical system may then be modeled as a sequence of physical processes, such as translations and refractions. The individual matrices are multiplied together in the correct operational order to predict ray paths through the entire system. For example, the lens shown in Figure 1 may be characterized by a matrix as follows: let the first and second refractions be represented by matrices R_1 and R_2, and the translation through the body of the lens be represented by a matrix T, where R_1 and R_2 are of the form M_2 and T is of the form M_1. The system matrix for the lens, which we will call M_{lens} is defined as: $M_{lens} = R_2 \cdot T \cdot R_1$. This matrix contains all of the information necessary to describe the lens. The simplest lens matrix is associated with a perfect thin lens of focal length *f*, is as follows:

$$M_{thin} = \begin{bmatrix} 1 & 0 \\ -\frac{1}{f} & 1 \end{bmatrix}.[3, p. 70]$$

3. The System Ray Transfer Matrix and Its Elements

A complete optical system is described by an input plane, where rays originate, a sequence of optical operations, and an output plane, where the ray pattern is analyzed. Thus the complete system representation contains two additional translation matrices that represent the rays' path from the system input plane to the first interface, and from the last interface to the system output plane. If translation from the origin to the first interface is represented by T_{in} and the translation from the second interface to the output plane is represented by T_{out}, the system matrix (M_{sys}) for the system shown in Figure 1 will be: $M_{sys} = T_{out} \cdot R_2 \cdot T \cdot R_1 \cdot T_{in}$. The optical system matrix elements are constrained values for certain applications, such as finite-conjugate imaging, and can be used to determine the location of cardinal points.

A general system matrix will be of the form:

$$M = \begin{bmatrix} A & B \\ C & D \end{bmatrix}.$$

When a finite-conjugate image is being formed at the output plane, matrix element $B \equiv 0$, and A is the linear, or transverse, magnification of the system.[3, pp. 72-73] These facts have been used to develop a method to experimentally determine the system matrix for real lenses. Once the matrix elements are known for a given lens, it is relatively simple to determine the lenses behavioral characteristics for various applications.

B. EXPERIMENTAL DETERMINATION OF MATRIX ELEMENTS

Given an unknown lens (or complex lens system), a general system matrix can be constructed by choosing arbitrary input and output planes and performing finite-conjugate imaging experiments. An initial ray translation from the input plane, or object, to the lens by a distance s_o is followed by transmission through the lens (represented by the lens matrix). Finally, there is translation to the image plane located a distance s_i from the lens. The matrix for this complete system will be,

$$M = \begin{bmatrix} A & B \\ C & D \end{bmatrix} = \begin{bmatrix} 1 & s_i \\ 0 & 1 \end{bmatrix} \cdot \begin{bmatrix} \alpha & \beta \\ \gamma & \delta \end{bmatrix} \cdot \begin{bmatrix} 1 & s_o \\ 0 & 1 \end{bmatrix} = \begin{bmatrix} \alpha + \gamma s_i & \beta + \delta s_i + (\alpha + \gamma s_i) s_o \\ \gamma & \delta + \gamma s_o \end{bmatrix}.$$

A, B, C, and D are the system matrix elements. As stated above, for finite-conjugate imaging B = 0, and A = linear magnification (m). α, β, γ, and δ are the lens matrix elements, from which the cardinal points may be determined. When the above system is solved for the lens matrix and the appropriate substitution made for the A and B elements the following system of equations is obtained.

$$\begin{aligned} \begin{bmatrix} \alpha & \beta \\ \gamma & \delta \end{bmatrix} &= \begin{bmatrix} 1 & s_i \\ 0 & 1 \end{bmatrix}^{-1} \cdot \begin{bmatrix} A & B \\ C & D \end{bmatrix} \cdot \begin{bmatrix} 1 & s_o \\ 0 & 1 \end{bmatrix}^{-1} \\ &= \begin{bmatrix} 1 & -s_i \\ 0 & 1 \end{bmatrix} \cdot \begin{bmatrix} m & 0 \\ C & D \end{bmatrix} \cdot \begin{bmatrix} 1 & -s_o \\ 0 & 1 \end{bmatrix} \\ &= \begin{bmatrix} m - C s_i & -D s_i - (m - C s_i) s_o \\ C & D - C s_o \end{bmatrix}. \end{aligned}$$

Each lens matrix element can now be expressed as a function of the system matrix elements, image distance (s_i), object distance (s_o), and linear magnification (m):

$$\begin{aligned} &\alpha = m - C s_i, \\ &\beta = -D s_i - (m - C s_i) s_o, \\ &\gamma = C, \ and \\ &\delta = D - C s_o. \end{aligned}$$

The next step in the development of an experimental procedure involves reducing the number of variables in the equations above to allow expression of the lens matrix elements in terms of readily measurable quantities. Since each of the lens matrix elements is necessarily constant their derivatives with respect to s_o and s_i must equal zero. Image distance (s_i) is assumed to be the independent variable and object distance (s_o) and linear magnification (m) the dependent variables for the purposes of these calculations. Then,

$$\frac{d\alpha}{ds_i} = \frac{dm}{ds_i} - C = \frac{dm}{ds_i} - \gamma = 0, \textit{ so that}$$

$$\gamma = \frac{dm}{ds_i},$$

$$\textit{and } \alpha = m - s_i \frac{dm}{ds_i}.$$

Next, the δ equation is solved for D and substituted into the β equation, giving

$$\beta = -(\delta + \gamma s_o)s_i - (m - \gamma s_i)s_o = -\delta s_i - ms_o,$$

$$\frac{d\beta}{ds_i} = -\delta - m\frac{ds_o}{ds_i} - s_o\frac{dm}{ds_i} = 0,$$

$$\delta = -m\frac{ds_o}{ds_i} - s_o\frac{dm}{ds_i}, \textit{ and}$$

$$\beta = m\left(s_i\frac{ds_o}{ds_i} - s_o\right) + s_o s_i\frac{dm}{ds_i}.$$

Each of the lens matrix elements has been expressed in terms of variables that can be measured. In order to verify these equations a 'thought experiment' will be performed in two steps. These expressions will first be validated algebraically using the familiar Gaussian thin lens formula. After confidence has been gained in the mathematics behind this method, a set of data will be generated using the thin lens formulae and evaluated to test the methods utility.

C. THE THOUGHT EXPERIMENT

1. Algebraic Validation of the Procedure

This portion of the thought experiment involved solving the thin lens formula for each of the variables in the equations derived above for the lens matrix elements. After the variables were determined, they were substituted into the matrix element equations to verify that the expected thin lens matrix resulted. The thin lens equations are,

$$\frac{1}{f} = \frac{1}{s_i} + \frac{1}{s_o}, \; and$$

$$m = -\frac{s_i}{s_o}.$$

Expressions are needed for s_i, s_o, m, and the derivatives of s_o and m with respect to s_i. Before the magnification derivative can be taken however, m should be cast only in terms of s_i:

$$s_i = \frac{fs_o}{s_o - f},$$

$$s_o = \frac{fs_i}{s_i - f}, \; and$$

$$m = \frac{fs_i - s_i^2}{fs_i}.$$

$$\frac{ds_o}{ds_i} = \frac{(s_i - f)f - fs_i}{(s_i - f)^2} = \frac{-f^2}{(s_i - f)^2}, \; and$$

$$\frac{dm}{ds_i} = \frac{fs_i(f - 2s_i) - (fs_i - s_i^2)f}{(fs_i)^2} = -\frac{1}{f}.$$

These expressions will be used to show that each lens matrix element equation gives the expected result for a thin lens.

$$\alpha = m - s_i \frac{dm}{ds_i} = -\frac{s_i}{s_o} - s_i\left(-\frac{1}{f}\right) = -\frac{s_i(s_i - f)}{fs_i} + \frac{s_i}{f} = \frac{fs_i - s_i^2 + s_i^2}{fs_i} = 1,$$

$$\beta = m\left(s_i \frac{ds_o}{ds_i} - s_o\right) + s_o s_i \frac{dm}{ds_i} = -\frac{s_i}{s_o}\left(\frac{-s_i f^2}{(s_i - f)^2} - s_o\right) - \frac{s_o s_i}{f} = -\frac{s_i}{s_o}\left(\frac{-s_i f^2 s_o^2}{f^2 s_i^2} - s_o\right) - \frac{s_o s_i}{f}$$

$$= \frac{s_i s_o^2}{s_o s_i} + s_i - \frac{s_o s_i}{f} = s_o + s_i - (s_o + s_i) = 0,$$

$$\gamma = \frac{dm}{ds_i} = -\frac{1}{f},\ and$$

$$\delta = -m\frac{ds_o}{ds_i} - s_o\frac{dm}{ds_i} = \frac{s_i}{s_o}\left(\frac{-f^2}{(s_i - f)^2}\right) + \frac{s_o}{f} = \frac{s_i}{s_o}\left(\frac{-f^2 s_o^2}{f^2 s_i^2}\right) + \frac{s_o}{f} = \frac{s_o}{f} - \frac{s_o}{s_i} = \frac{s_o(s_i - f)}{f s_i} = \frac{s_o}{s_o} = 1.$$

Therefore,

$$\begin{bmatrix} \alpha & \beta \\ \gamma & \delta \end{bmatrix} = \begin{bmatrix} 1 & 0 \\ -\frac{1}{f} & 1 \end{bmatrix},$$

as expected. This indicates that the procedure is valid.

2. Utility Verification

As previously stated the purpose of this portion of the thought experiment is to determine if the method of determining the lens matrix elements described above will be practically achievable. The following simulation was performed: artificial data were generated in Microsoft Excel using the ideal thin lens formula for a hypothetical 5 cm positive thin lens. Image distance was chosen as the independent variable and assigned values from 10 to 30 cm in 1 cm increments. Object distance was calculated from the ideal focal length and image distance values. Linear magnification was then calculated for each image and object distance set. The derivatives of magnification and image distance with respect to object distance were estimated by calculating the differences between magnification, image distance, and object distance as shown below.

$$\frac{dm}{ds_o} \approx \frac{\Delta m}{\Delta s_o},\ and$$

$$\frac{ds_i}{ds_o} \approx \frac{\Delta s_i}{\Delta s_o}.$$

These ratios were then plotted against an average value for object distance. Data were imported into Matlab and least-squares fitted to a user-defined function using the 'lsqcurvefit' function. The user-defined functions were defined by taking the appropriate derivatives of the thin lens equation and are as follows:

$$\frac{ds_i}{ds_o} = \frac{-f^2}{(s_o - f)^2}, \textit{ and}$$
$$\frac{dm}{ds_o} = \frac{f}{(s_o - f)^2}.$$

Each function is fitted to the data, which is formatted in (x,y) pairs, by determining the best value for the focal length *f*. After the focal length is determined, values for image distance, magnification, and the derivatives of object distance and magnification with respect to image distance are calculated. These values are then used to calculate the lens matrix elements using the relationships derived earlier. The simulated lens matrix is then constructed from their mean values. To ensure that the curve generated is a reasonable fit to the collected data both are plotted on the same graph, shown in Figure 2.

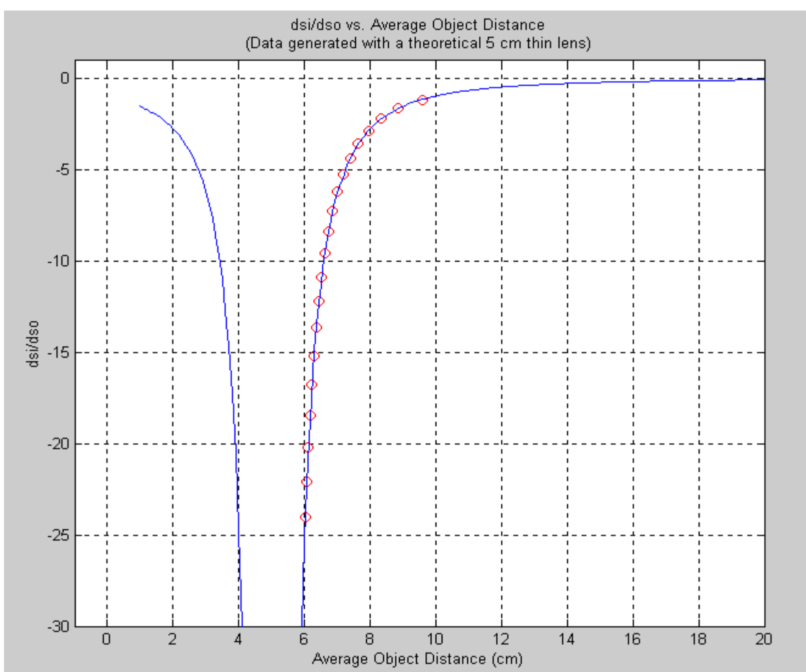

Figure 2. Plot of ds_i/ds_o vs. s_o, data and fitted curve for a hypothetical 5 cm thin lens.

3. Offset Measurements

Actual complex lens systems have finite thickness. Hence the question arises pertaining to the locations of appropriate origins from which to measure object and image distances. Since measurements will all be made from the same points with respect to the lens system and image and object planes there will be no effect on the differential values Δm, Δs_i, and Δs_o used to estimate the derivatives. This constant offset between the point of measurement of object distance and the actual location of the object (Δ) is accounted for by incorporating it into the function that is used to fit the data. The new function is as follows:

$$\frac{ds_i}{ds_o} = \frac{-f^2}{(s_o - \Delta - f)^2}\ .$$

Where ds_i/ds_o is the unchanged y-axis data, s_o is the offset x-axis data, and Δ and f are the variables being calculated. A simulation of Δ was incorporated into the thought experiment data by artificially adding 2.4 cm to each simulated s_o data point. Results for f, Δ, and the calculated thin lens matrix (M_{thin}) closely match the expected values and are shown below:

$$f = 5.0072,\ \Delta = 2.3915,\ \text{and}$$

$$M_{thin} = \begin{bmatrix} 1.0000 & 0.0000 \\ -0.1997 & 1.0000 \end{bmatrix}.$$

D. VALIDATION USING A REAL THIN LENS

The logical next step in this set of experiments is to collect and analyze data on a real thin lens to ensure that the technique works in practice. Data were collected and analyzed for a thin glass lens whose nominal focal length was known a priori to be about 10 cm.

1. Experimental Setup

This experiment was set up on a standard optical bench. A light source with a cross type pattern was placed on the right hand side of the bench. The surface of this light source was defined as the object plane. An image was formed on a small sheet of frosted glass placed on the left hand side of the bench and the lens was placed between the object and image planes. Measurements were made from the center of the lens to the surfaces of the frosted glass and the light source. Defining image and object distance in this way most closely approximates the parameters for an ideal thin lens.

2. Data and Results

The data collected from this experiment is located in appendix A. After the initial calculations were performed it became clear that some anomalous data points were causing inaccurate results. Spurious data points were identified and eliminated. All derivative data whose values were less than or equal to -5 were discarded. Additionally, the asymptotic s_o data above 40 cm did not contribute any significant information and so were discarded. Figure 3 is a plot of all collected data and graphically shows which data points were discarded.

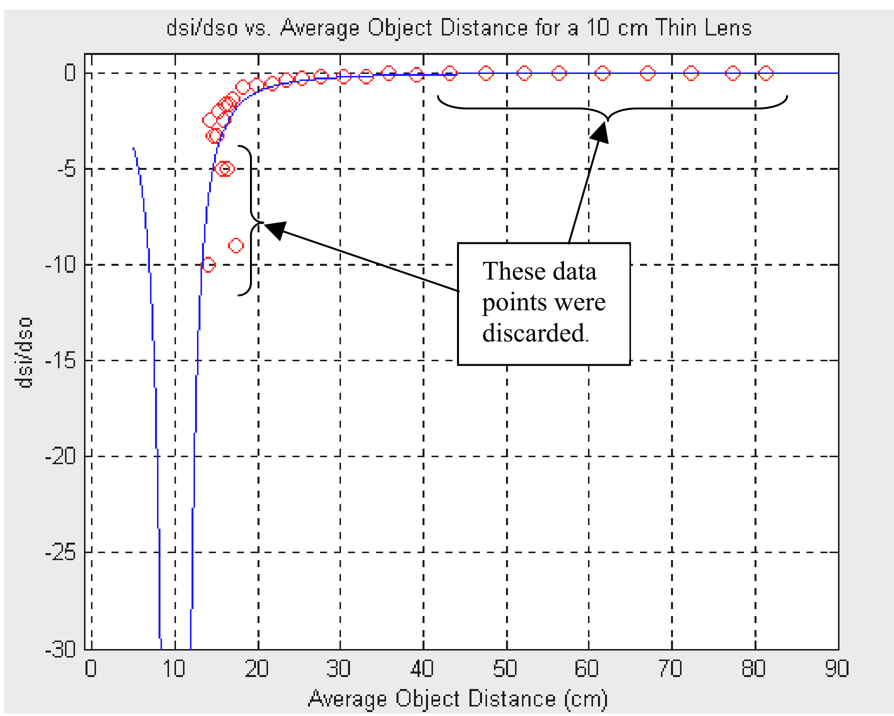

Figure 3. Plot of ds_i/ds_o vs. s_o, data and fitted curve for a 10 cm thin lens.

Initially this data set looked acceptable and returned credible results. The resulting focal length was 10.085 cm, close to the expected value. However, when the average object distance data were artificially offset, as in the thought experiment, the calculated focal length was slightly greater than 7 cm, substantially different from the expected value. This difference is due to inaccuracies in measurement while taking data. While the actual distances were measured to within a millimeter, the error associated with light source and lens positioning required for image formation was much greater as object distance approached the lens' focal length. After the indicated data were discarded the following results were obtained:

$$M_{thin} = \begin{bmatrix} 1.0000 & 0.0000 \\ -0.1021 & 1.0000 \end{bmatrix} \quad , and$$
$$Calculated\ Offset \ = \ -0.9197$$

$$M_{offset} = \begin{bmatrix} 1.0000 & 0.0000 \\ -0.1021 & 1.0000 \end{bmatrix} \quad .$$
$$Calculated\ Offset \ = \ 4.0874\ cm$$

Initial calculations on the retained data were performed using the function that assumed no offset. Focal length yielded from the first set of calculations was 9.2332 cm. While somewhat lower than expected this value was accepted as a reasonable validation of the technique. Results from the data after a 5 cm offset had been applied were as seen above. The calculated offset was about 1 cm less than expected, and the focal length was approximately 6 mm greater than the previous result. The most likely cause of this discrepancy was related to the assumption that the principal planes for the thin lens were located at the center of the lens. An ideal thin lens is assumed to be infinitesimally thin, with all of its cardinal points co-located on the lens plane. This is obviously not the case with a real thin lens of finite thickness but becomes a good assumption as image and object distances become large compared to the focal length of the lens. The calculated focal lengths agree to within a millimeter for the two cases shown above, when the offset function is used to fit both sets of data. Additionally, when the calculated offsets are combined the artificially entered offset of 5 cm is recovered, as expected.

The thin lens thought experiment simulations and laboratory data analysis were deemed successful and a validation of the technique for determining the lens matrix.

THIS PAGE INTENTIONALLY LEFT BLANK

III. DETERMINATION OF MATRIX ELEMENTS FOR COMPLEX OPTICAL SYSTEMS

A. COMPLEX LENS SYSTEM SIMULATIONS

Similar to the previous thought experiments, a notional complex lens system was 'designed' to verify that the lens system matrix elements could be calculated from measurable data. The first complex lens system was comprised of three thin lenses with constant separations. Its nominal input and output planes were located at the outside faces of the individual lenses that comprised the system (see Figure 4). A second complex lens system was considered which incorporated idealized offsets at each end of the system. This second hypothetical system is shown in Figure 5. These mental constructs were used to verify that the matrix element determination method could be trusted to analyze actual data taken on the LINUS lenses.

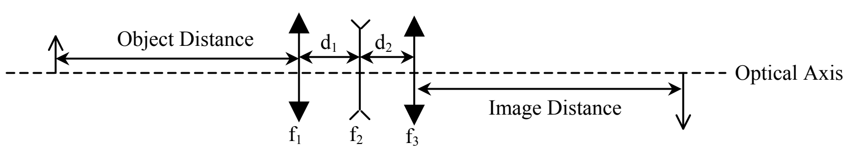

Figure 4. First notional complex lens system.

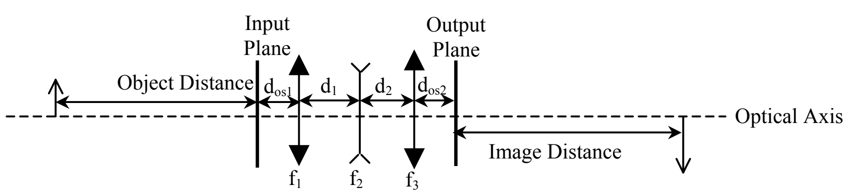

Figure 5. Second notional complex lens system.

1. Data Generation for the Simulations

Each of the complex systems above has a characteristic matrix. Using the nomenclature M_1, M_2, and M_3 for the component thin lens matrices, T_1, and T_2 for the lens separation matrices, and T_{O1}, and T_{O2} for the outer offset matrices, we can predict the system matrices for each complex lens system as follows:

$$
\begin{aligned}
M_{system_1} &= M_3 \cdot T_2 \cdot M_2 \cdot T_1 \cdot M_1 \\
&= \begin{pmatrix} 1 & 0 \\ -\frac{1}{f_3} & 1 \end{pmatrix} \cdot \begin{pmatrix} 1 & d_2 \\ 0 & 1 \end{pmatrix} \cdot \begin{pmatrix} 1 & 0 \\ -\frac{1}{f_2} & 1 \end{pmatrix} \cdot \begin{pmatrix} 1 & d_1 \\ 0 & 1 \end{pmatrix} \cdot \begin{pmatrix} 1 & 0 \\ -\frac{1}{f_1} & 1 \end{pmatrix} \\
&= \begin{pmatrix} \frac{f_2 - d_2}{f_2} + \frac{d_1 d_2 - d_1 f_2 - d_2 f_2}{f_1 f_2} & \frac{d_1 f_2 + d_2 f_2 - d_1 d_2}{f_2} \\ \frac{d_2 - f_3 - f_2}{f_2 f_3} + \frac{d_1 f_2 + d_1 f_3 + d_2 f_2 - f_2 f_3 - d_1 d_2}{f_1 f_2 f_3} & \frac{d_1 d_2 - d_1 f_2 - d_1 f_3 + f_2 f_3 - d_2 f_2}{f_2 f_3} \end{pmatrix} \\
&= \begin{pmatrix} \alpha & \beta \\ \gamma & \delta \end{pmatrix}, \ and
\end{aligned}
$$

$$
\begin{aligned}
M_{system_2} &= T_{O2} \cdot M_3 \cdot T_2 \cdot M_2 \cdot T_1 \cdot M_1 \cdot T_{O1} \\
&= \begin{pmatrix} 1 & d_{os_2} \\ 0 & 1 \end{pmatrix} \cdot \begin{pmatrix} 1 & 0 \\ -\frac{1}{f_3} & 1 \end{pmatrix} \cdot \begin{pmatrix} 1 & d_2 \\ 0 & 1 \end{pmatrix} \cdot \begin{pmatrix} 1 & 0 \\ -\frac{1}{f_2} & 1 \end{pmatrix} \cdot \begin{pmatrix} 1 & d_1 \\ 0 & 1 \end{pmatrix} \cdot \begin{pmatrix} 1 & 0 \\ -\frac{1}{f_1} & 1 \end{pmatrix} \cdot \begin{pmatrix} 1 & d_{os_1} \\ 0 & 1 \end{pmatrix} \\
&= \begin{pmatrix} \alpha & \beta \\ \gamma & \delta \end{pmatrix}.
\end{aligned}
$$

The expanded form of $M_{system2}$ is not shown because of its size. Hypothetical values defined for focal length, separation distance, and offset distance are shown in Table 1.

f_1	20 cm
f_2	-40cm
f_3	25 cm
d_1	0.5 cm
d_2	0.5 cm
d_{os1}	0.6 cm
d_{os2}	1.2 cm

Table 1. Hypothetical values for the notional systems shown in Figures 4 and 5.

The following system matrices were calculated based on the hypothetical values given in Table 1.

$$M_{system_1} = \begin{pmatrix} 0.9322 & 1.0063 \\ -0.0641 & 0.9722 \end{pmatrix}, \; and$$

$$M_{system_2} = \begin{pmatrix} 0.8853 & 2.7041 \\ -0.0641 & 0.9338 \end{pmatrix}.$$

When these lens system matrices are appropriately combined with the transfer matrices associated with the object and image distances the optical system matrix is obtained. The 'B' element of this matrix is, by definition, equal to zero since a finite-conjugate image is being formed. A direct relationship between image and object distance is revealed as shown below.

$$M_{optical\ system} = \begin{pmatrix} 1 & s_i \\ 0 & 1 \end{pmatrix} \cdot M_{lens\ system} \cdot \begin{pmatrix} 1 & s_o \\ 0 & 1 \end{pmatrix}, \; and$$

$$s_o = -\frac{1.0063 + 0.9722 \cdot s_i}{0.9622 - 0.0641 \cdot s_i}$$

for the lens system shown in Figure 4.

A similar relationship follows for the second lens system. Data were generated by incrementing the simulated image distance from 15.01 to 50 cm in 0.01 cm increments and calculating the subsequent object distances per the formula above. Comparable image and object distances were expected to be measurable in the laboratory for various wavelengths of light. From these measurements the change in image distance with respect to the change in object distance can be determined and plotted against the average object distance, as was the case for the thin lens, as described in Chapter II.

2. Matrix Element Determination

The data generated in the simulations were plotted and fitted to the same function used before for the thin lens with a constant offset. Ideally, this method should return the focal length of the complex lens as measured from the adjacent principle plane and the distance between the input plane and that principle plane (f_1 and r, respectively, as shown in Figure 6). Figure 6 [adapted from ref. 3, p. 75] and Table 2 [adapted from ref. 3, p. 77] show the geometric relationships between lens system matrix elements, system focal lengths (F), principle planes (H), and input and output planes. The nodal points N_1 and N_2 are not shown.

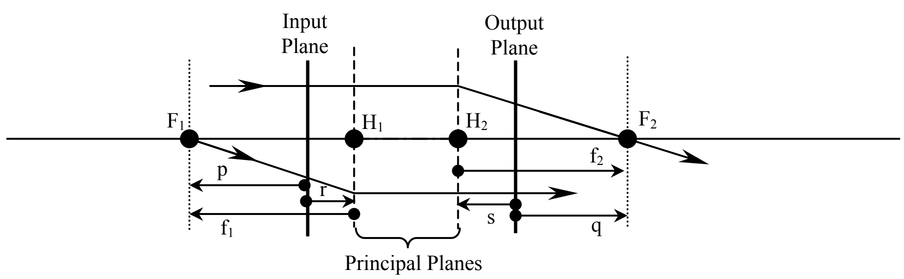

Figure 6. Locations of cardinal points F_1, F_2, H_1, and H_2 in a complex optical system.

$$p = \frac{\delta}{\gamma}$$

$$q = \frac{\alpha}{\gamma}$$

$$r = \frac{\delta - 1}{\gamma}$$

$$s = \frac{1 - \alpha}{\gamma}$$

Measured from input and output planes

$$f_1 = p - r = \frac{1}{\gamma}$$

$$f_2 = q - s = -\frac{1}{\gamma}$$

Measured from principal planes

Table 2. Cardinal point locations defined in terms of lens system matrix elements.

Note that β cannot be determined using these relationships. However, recalling that the optical system and lens system matrix determinants must equal the ratio of the indices of refraction of the media at the system's input and output, which is one for this experiment, β can be determined once the other matrix elements are known.

Results from the data generated for these notional lens systems were as expected. The least squares curve-fitting function returned $-f_1$ and $-r$ from which, γ and δ were determined. Since the relationship between r and s involves three unknowns and two equations there is no way to determine α with only the data at hand. It was determined that a second set of data in the reverse direction through the lens would return the values necessary for calculating α.

The 'reverse' data set was generated using a relationship between image and object distance similar to the one used while generating the first set. The relationship was obtained by determining a new lens system matrix and then following the same procedure as previously discussed. The forward and reverse lens matrices are very closely related, as shown below using those from the second notional system.

$$M_{lens_f} = \begin{pmatrix} 0.8853 & 2.7041 \\ -0.0641 & 0.9338 \end{pmatrix}, \ and$$
$$M_{lens_r} = \begin{pmatrix} 0.9338 & 2.7041 \\ -0.0641 & 0.8853 \end{pmatrix}.$$

This second data set returned $-f_2$ and $-s$, from which α and a second value for γ were calculated. The second determination of γ provides an indication of an appropriate level of confidence in the measured data. If the two values are very close then a high level of confidence is warranted. After analysis was completed on the generated data the following results were seen:

$$M_{known} = \begin{pmatrix} 0.8853 & 2.7041 \\ -0.0641 & 0.9338 \end{pmatrix}, \ and$$
$$M_{calculated} = \begin{pmatrix} 0.8852 & 2.7042 \\ -0.0641 & 0.9338 \end{pmatrix}.$$

The consistency is excellent.

B. LINUS CAMERA OBJECTIVE CHARACTERIZATION IN VISIBLE LIGHT

LINUS' lens systems are aplanats comprised of two and three individual lenses of unknown composition with unknown surface curvatures and element separations placed in black barrel mounts. Each barrel is marked only with regard to the proper light propagation direction. The lenses are coated with an anti-reflective material designed for optimum throughput at near-ultraviolet wavelengths. The camera objective for LINUS was initially characterized experimentally using four different colors of visible light. In these experiments, object distance was treated as the independent variable and shortened in 0.5 cm increments from a maximum value of 26 cm down to 12 cm. As can be seen in Figure 3, the most critical data points are those near the 'knee' of the ds_i/ds_o vs. s_o curve since they essentially define the curve. Data was collected using red, yellow, green, and blue-green band pass filters and analyzed using the techniques previously discussed.

During initial data collection and analysis it was discovered that the anti-reflective lens coating did not work at the visible wavelengths. Lens flare, due to multiple reflections inside the lens system, resulted in four images being formed by the system instead of one. One image was virtual and the other three were real. The first real image was very close to the output plane and could be disregarded. The two remaining images were separated by approximately 1 cm and it could not be readily determined which was the desired image and which was an artifact of the lens flare. Consequently data were taken and analyzed for both sets of images. Subsequent data analysis revealed that the images farthest from the output plane returned focal lengths as measured from the principal planes that were consistent while the images closer to the output plane returned inconsistent values. This fact indicated that the image closer to the output plane was an artifact of lens flare and should be neglected.

1. Red Filter Results

Data taken using the red filter resulted in a focal length from the principal planes of 10.98 cm, a forward focal length of 9.15 cm, and a reverse focal length of 7.7 cm. The lens system matrix was:

$$M_{red} = \begin{pmatrix} 0.8328 & 4.5682 \\ -0.0910 & 0.7014 \end{pmatrix}.$$

2. Yellow Filter Results

Data taken using the yellow filter resulted in a focal length from the principal planes of 10.34 cm, a forward focal length of 9.5 cm, and a reverse focal length of 8.17 cm. The lens system matrix was:

$$M_{yellow} = \begin{pmatrix} 0.9188 & 2.8301 \\ -0.0967 & 0.7904 \end{pmatrix}.$$

3. Green Filter Results

Data taken using the green filter resulted in a focal length from the principal planes of 10.37 cm, a forward focal length of 9.56 cm, and a reverse focal length of 8.08 cm. The lens system matrix was:

$$M_{green} = \begin{pmatrix} 0.9226 & 2.9095 \\ -0.0965 & 0.7797 \end{pmatrix}.$$

4. Blue-Green Filter Results

Data taken using the blue-green filter resulted in a focal length from the principal planes of 10.8 cm, a forward focal length of 9.33 cm, and a reverse focal length of 7.77 cm. The lens system matrix was:

$$M_{blue-green} = \begin{pmatrix} 0.8636 & 4.0966 \\ -0.0926 & 0.7188 \end{pmatrix}.$$

THIS PAGE INTENTIONALLY LEFT BLANK

IV. DETERMINATION OF MATRIX ELEMENTS FOR THE LINUS PRIMARY AND CAMERA OBJECTIVE LENSES AT ULTRAVIOLET WAVELENGTHS

A. EXPERIMENTAL SETUP

This portion of the thesis experiment was performed using a platinum hollow cathode lamp to illuminate a simple sewing needle. The shadow image of the needle was then focused onto the image intensifier of LINUS's UV camera through a band-pass filter. A photograph of the experimental layout is shown in Figure 7.

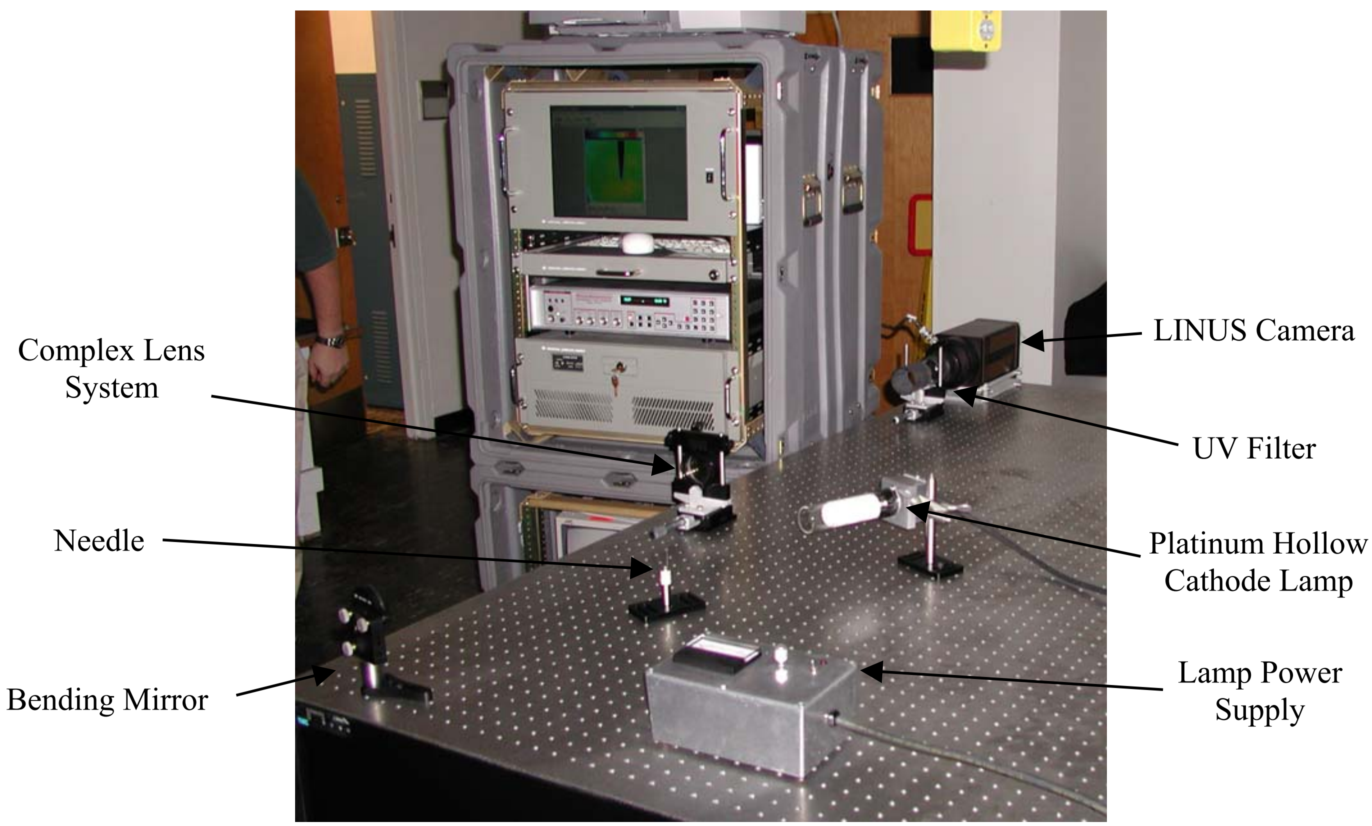

Figure 7. Physical layout used for measurements taken with the camera objective lens.

WinView32, a Windows-based image acquisition and camera control program provided by the camera manufacturer, provided the user-camera interface to allow focusing of the needle. This program allows the user to control the exposure time for the camera, determine whether the image is inverted or normal, and control most of the other advanced features of the camera. For the purposes of this experiment the camera was run primarily in the 'focus' mode (a free-running multiple frame data acquisition mode) and exposure time was adjusted between 0.25 and 4 seconds as necessary to position the needle correctly for image formation. A screen capture of this interface with an image of the needle was taken and is shown in the figure below.

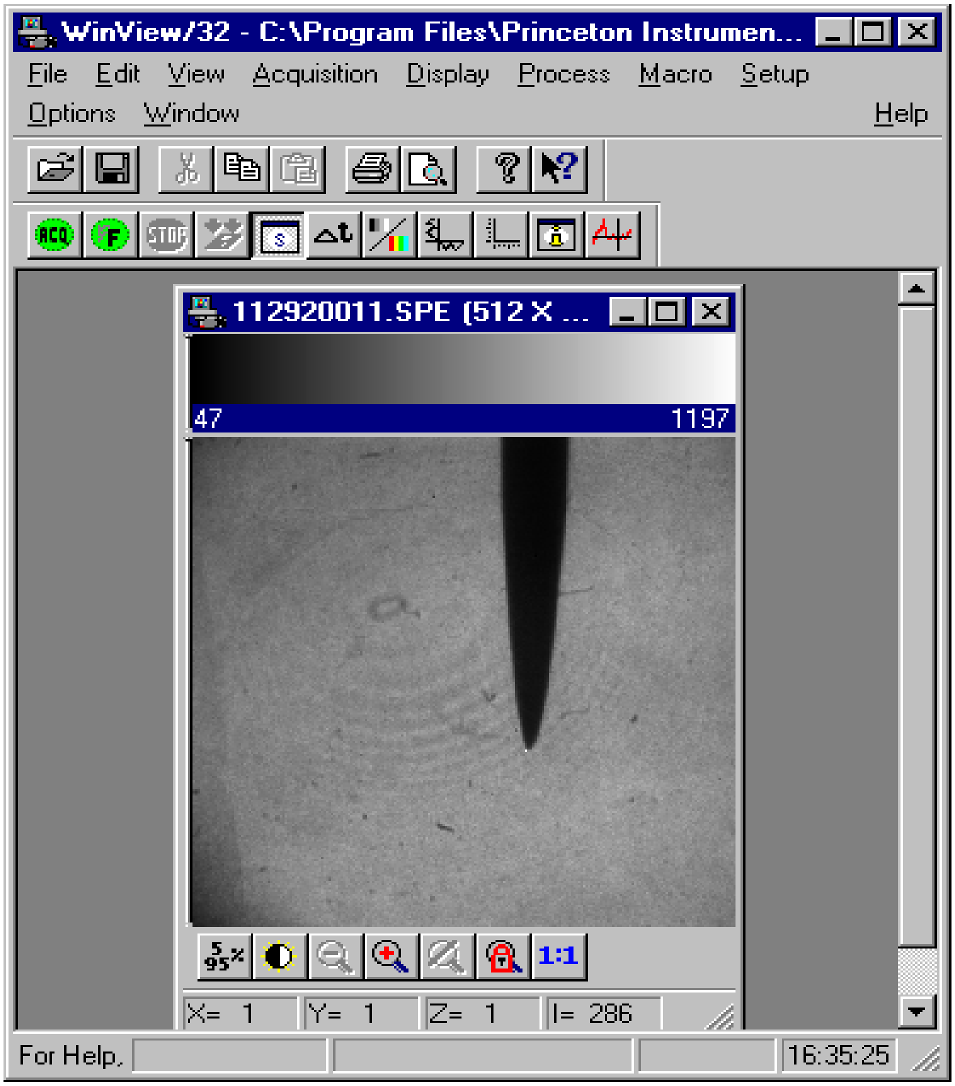

Figure 8. The camera interface program control window and a needle image.

B. DATA GENERATION AND ANALYSIS

Image distances were initially incremented in 1 cm steps to generate the corresponding object distances. As the change in object distance became less than unity the image distance increments were increased to 2, 3, and 4 cm. This technique was employed to reduce error propagation as the data were manipulated into the form required for computer analysis. Data was taken in the forward and reverse directions for both the camera and the primary objective lenses using four different ultraviolet filters centered at 220, 300, 334, and 370 nm with approximately 10 nm bandwidths.

Each data set was input to a spreadsheet for further manipulation. Offsets from the measurement points were accounted for and final values for object distance were generated. Next, values for Δs_i, Δs_o, average s_o, and $\Delta s_i/\Delta s_o$ were calculated. All of these data are included in Appendix A. The Matlab code generated to complete the analysis is included in Appendix B.

Initial analysis was performed using the method described in Chapter III and was found to be unsatisfactory. There was an excessive amount of data scatter in the $\Delta s_i/\Delta s_o$ vs. Avg. s_o plots, giving somewhat dubious results. In an effort to reduce the amount of uncertainty associated with analyzing the data, s_o was plotted against s_i and fit to a general hyperbolic function that would be expected from theoretical considerations. This function was then algebraically manipulated into the correct form, differentiated and used to generate values for ds_i/ds_o from object distance data. The function and its derivative are shown below.

$$s_o = \frac{as_i + b}{cs_i + d} \quad \rightarrow \quad s_i = \frac{ds_o - b}{a - cs_o},$$

from which,

$$\frac{ds_i}{ds_o} = \frac{ad - bc}{(cs_o - a)^2}.$$

Optimal values for a, b, c, and d were calculated by the Matlab curve fitting function 'lsqcurvefit' and then used with the object distance data already present to generate a refined data set. This data set was then fit using the function defined earlier, which returned the focal lengths as measured from the principal planes and the offset from the input and output planes. Values for forward and reverse focal length as measured from the respective barrel face and the lens system matrix were also calculated and returned.

C. RESULTS FOR THE PRIMARY OBJECTIVE LENS SYSTEM

1. 220 nm Wavelength

Data taken using the 220 nm bandpass filter resulted in focal lengths from the principal planes of 18.2 and 24.3 cm, a forward focal length of 18.9 cm, and a reverse focal length of 31.5 cm. The system lens matrix was:

$$M_{\text{Primary-220}} = \begin{pmatrix} 0.8883 & -6.7445 \\ -0.0471 & 1.4833 \end{pmatrix}.$$

Plots of image distance vs. object distance and ds_i/ds_o vs. object distance including the fitted curve are shown in Figure 9.

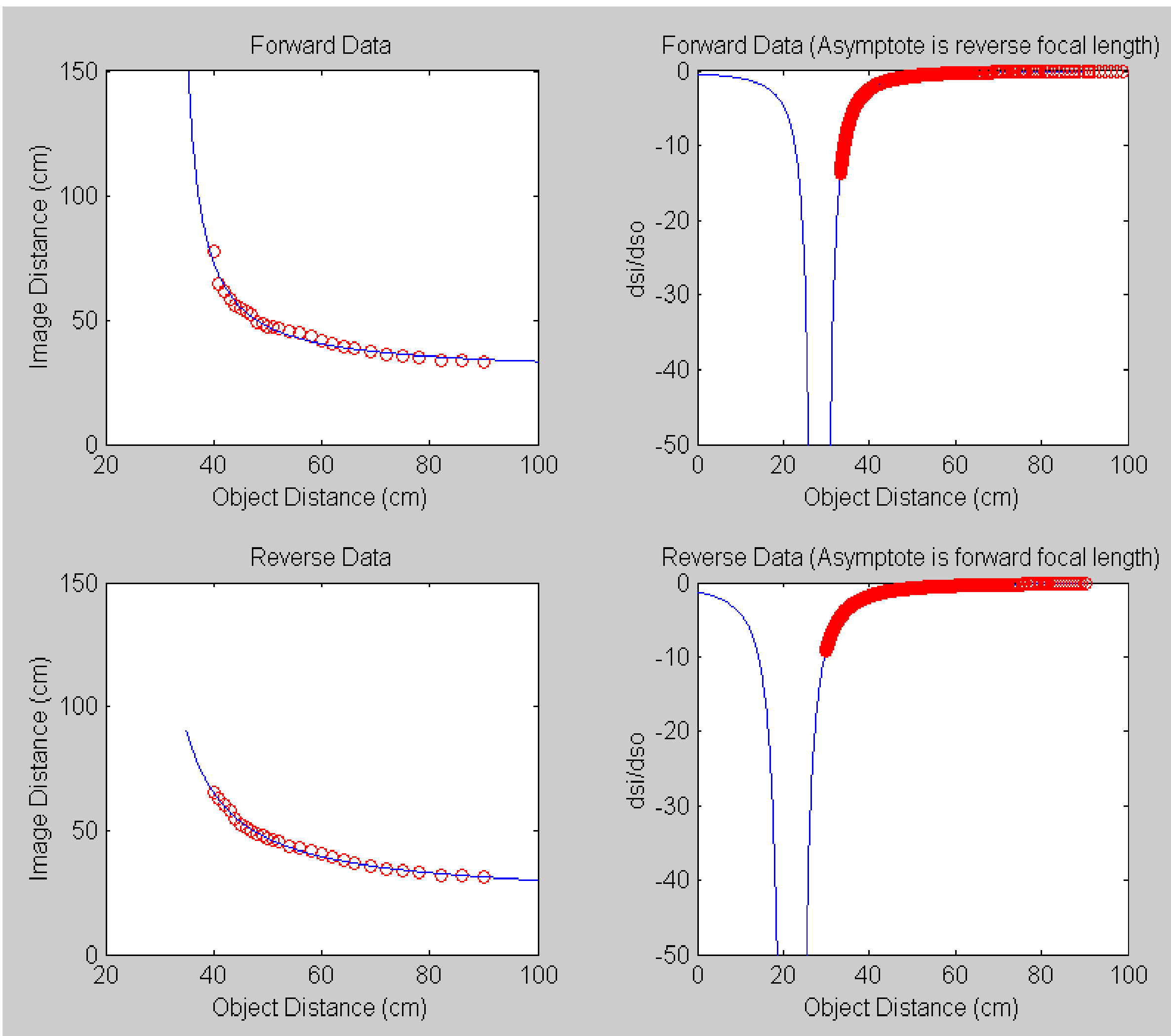

Figure 9. Plots of s_i vs. s_o and ds_i/ds_o vs. s_o for the primary objective at 220 nm.

2. 300 nm Wavelength

Data taken using the 300 nm bandpass filter resulted in focal lengths from the principal planes of 26.2 and 26.5 cm, a forward focal length of 23.4 cm, and a reverse focal length of 25.7 cm. The system lens matrix was:

$$M_{\text{Primary-300}} = \begin{pmatrix} 0.8903 & 3.4341 \\ -0.0380 & 0.9768 \end{pmatrix}.$$

Plots of image distance vs. object distance and ds_i/ds_o vs. object distance including the fitted curve are shown in Figure 10.

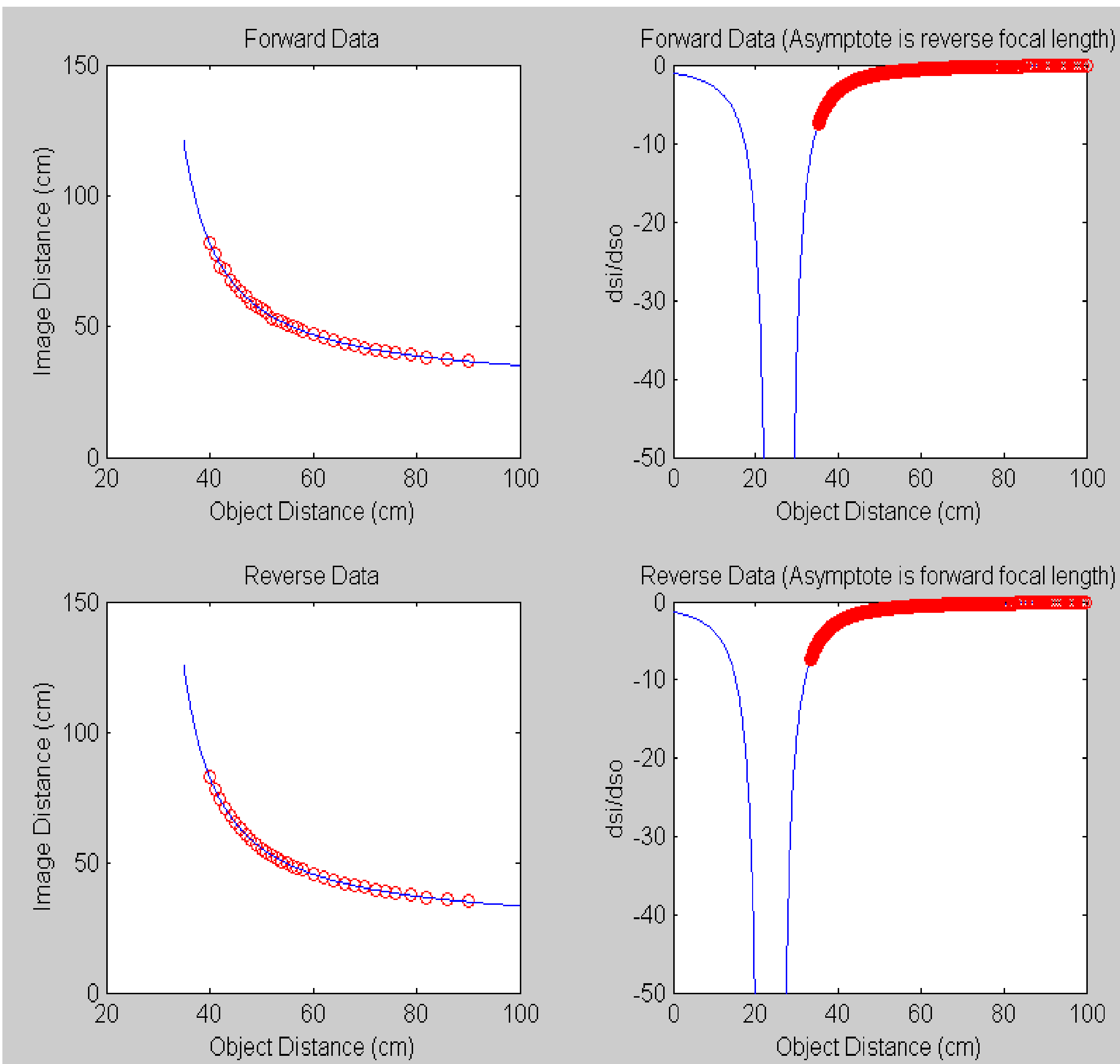

Figure 10. Plots of s_i vs. s_o and ds_i/ds_o vs. s_o for the primary objective at 300 nm.

3. 334 nm Wavelength

Data taken using the 334 nm bandpass filter resulted in focal lengths from the principal planes of 27.2 and 26.8 cm, a forward focal length of 24.1 cm, and a reverse focal length of 25.1 cm. The system lens matrix was:

$$M_{\text{Primary-334}} = \begin{pmatrix} 0.8916 & 4.6043 \\ -0.0370 & 0.9303 \end{pmatrix}.$$

Plots of image distance vs. object distance and ds_i/ds_o vs. object distance including the fitted curve are shown in Figure 11.

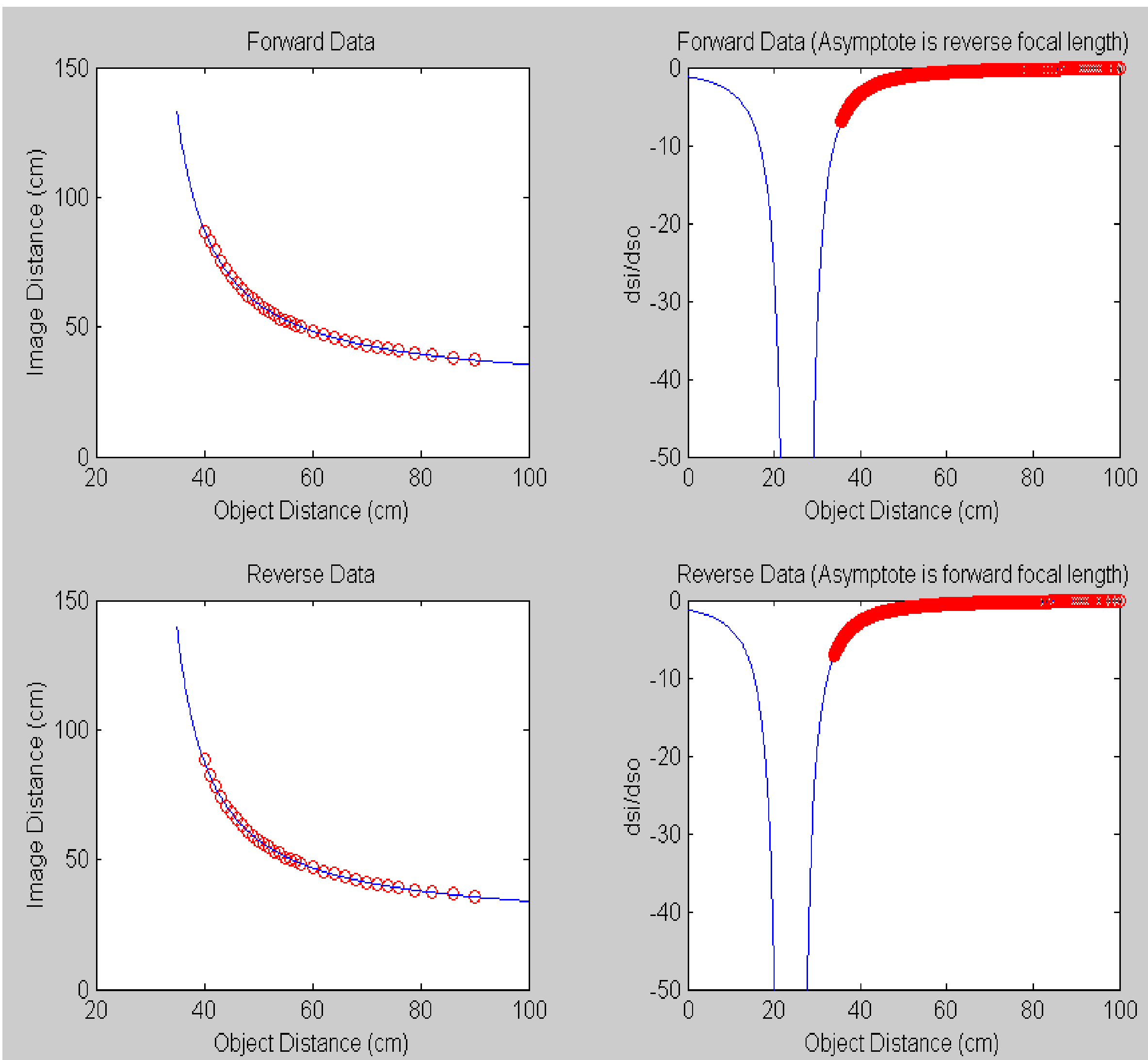

Figure 11. Plots of s_i vs. s_o and ds_i/ds_o vs. s_o for the primary objective at 334 nm.

4. 370 nm Wavelength

Data taken using the 370 nm bandpass filter resulted in focal lengths from the principal planes of 19.9 and 26.5 cm, a forward focal length of 21.4 cm, and a reverse focal length of 35.9 cm. The system lens matrix was:

$$M_{\text{Primary-370}} = \begin{pmatrix} 0.9242 & -10.0199 \\ -0.0431 & 1.5498 \end{pmatrix}.$$

Plots of image distance vs. object distance and ds_i/ds_o vs. object distance including the fitted curve are shown in Figure 12.

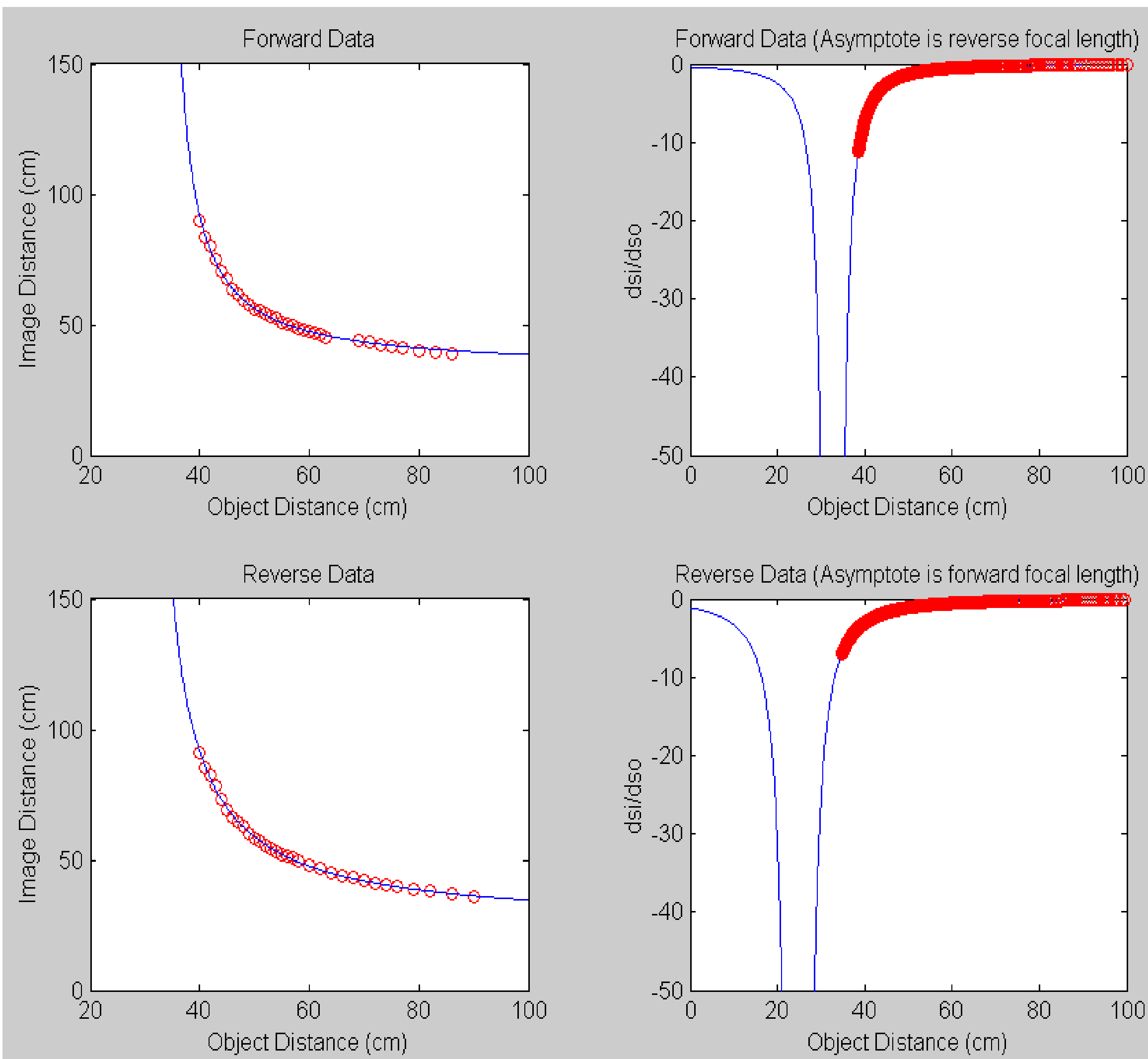

Figure 12. Plots of s_i vs. s_o and ds_i/ds_o vs. s_o for the primary objective at 370 nm.

D. RESULTS FOR THE CAMERA OBJECTIVE LENS SYSTEM

1. 220 nm Wavelength

Data taken using the 220 nm bandpass filter resulted in focal lengths from the principal planes of 48.5 and 39.8 cm, a forward focal length of 58.8 cm, and a reverse focal length of 41.8 cm. The system lens matrix was:

$$M_{\text{Camera-220}} = \begin{pmatrix} 1.3319 & -11.4763 \\ -0.0226 & 0.9460 \end{pmatrix}.$$

Plots of image distance vs. object distance and ds_i/ds_o vs. object distance including the fitted curve are shown in Figure 13.

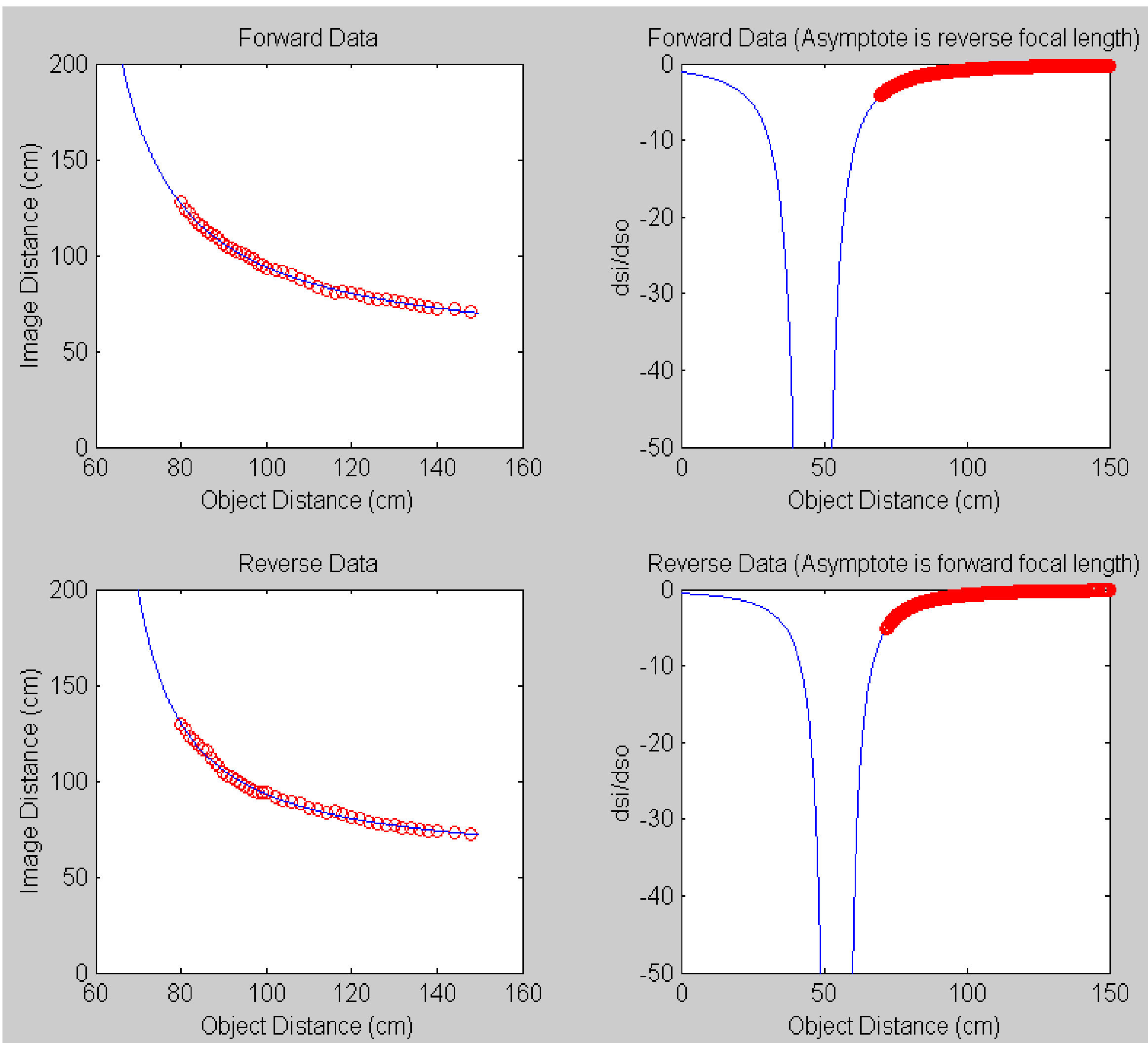

Figure 13. Plots of s_i vs. s_o and ds_i/ds_o vs. s_o for the camera objective at 220 nm.

2. 300 nm Wavelength

Data taken using the 300 nm bandpass filter resulted in focal lengths from the principal planes of 50.7 and 50.2 cm, a forward focal length of 53.0 cm, and a reverse focal length of 51.6 cm. The system lens matrix was:

$$M_{\text{Camera-300}} = \begin{pmatrix} 1.0493 & -3.7035 \\ -0.0198 & 1.0230 \end{pmatrix}.$$

Plots of image distance vs. object distance and ds_i/ds_o vs. object distance including the fitted curve are shown in Figure 14.

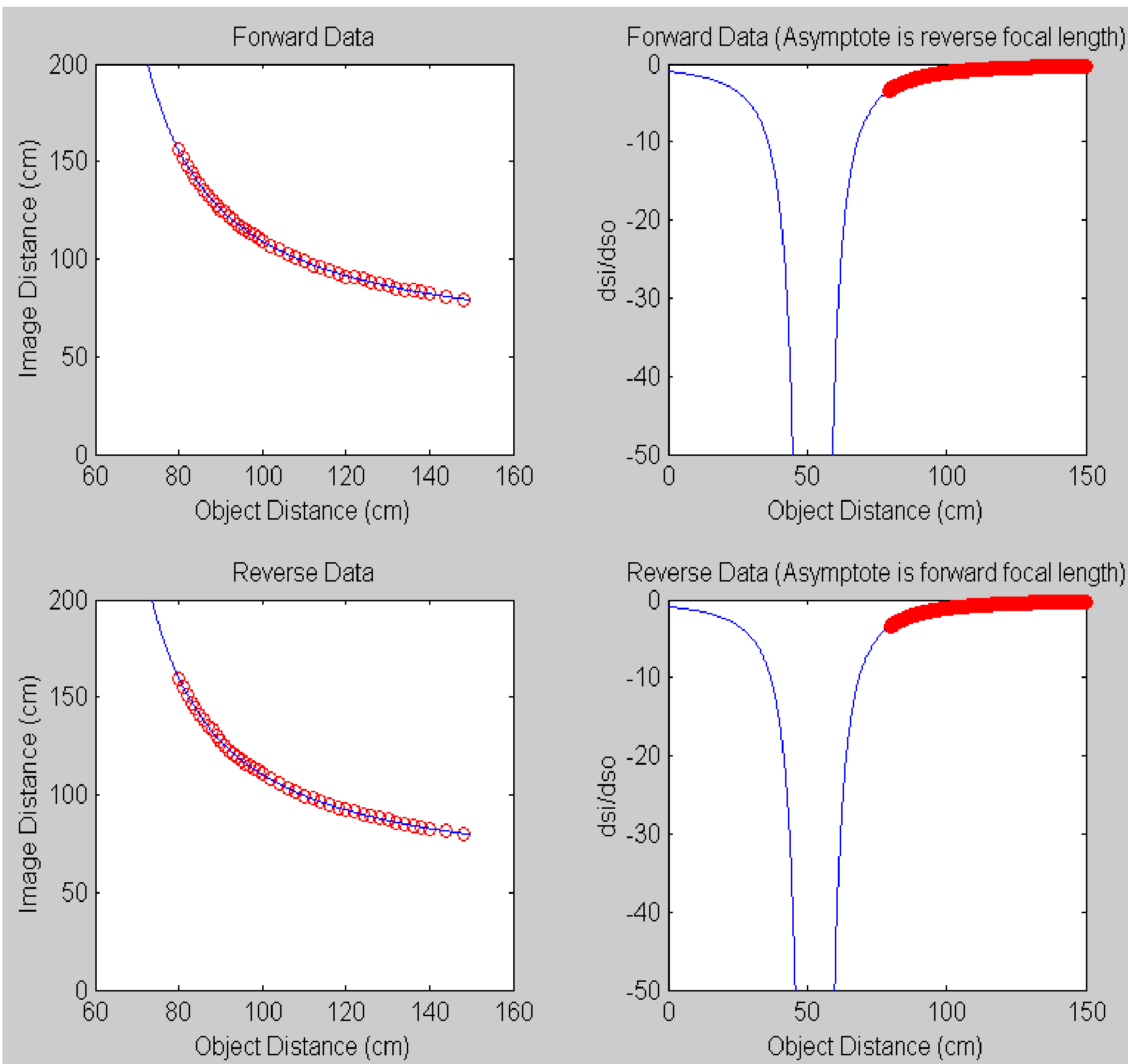

Figure 14. Plots of s_i vs. s_o and ds_i/ds_o vs. s_o for the camera objective at 300 nm.

3. 334 nm Wavelength

Data taken using the 334 nm bandpass filter resulted in focal lengths from the principal planes of 51.7 and 52.6 cm, a forward focal length of 52.0 cm, and a reverse focal length of 52.9 cm. The system lens matrix was:

$$M_{\text{Camera-334}} = \begin{pmatrix} 0.9968 & -0.5639 \\ -0.0192 & 1.0141 \end{pmatrix}.$$

Plots of image distance vs. object distance and ds_i/ds_o vs. object distance including the fitted curve are shown in Figure 15.

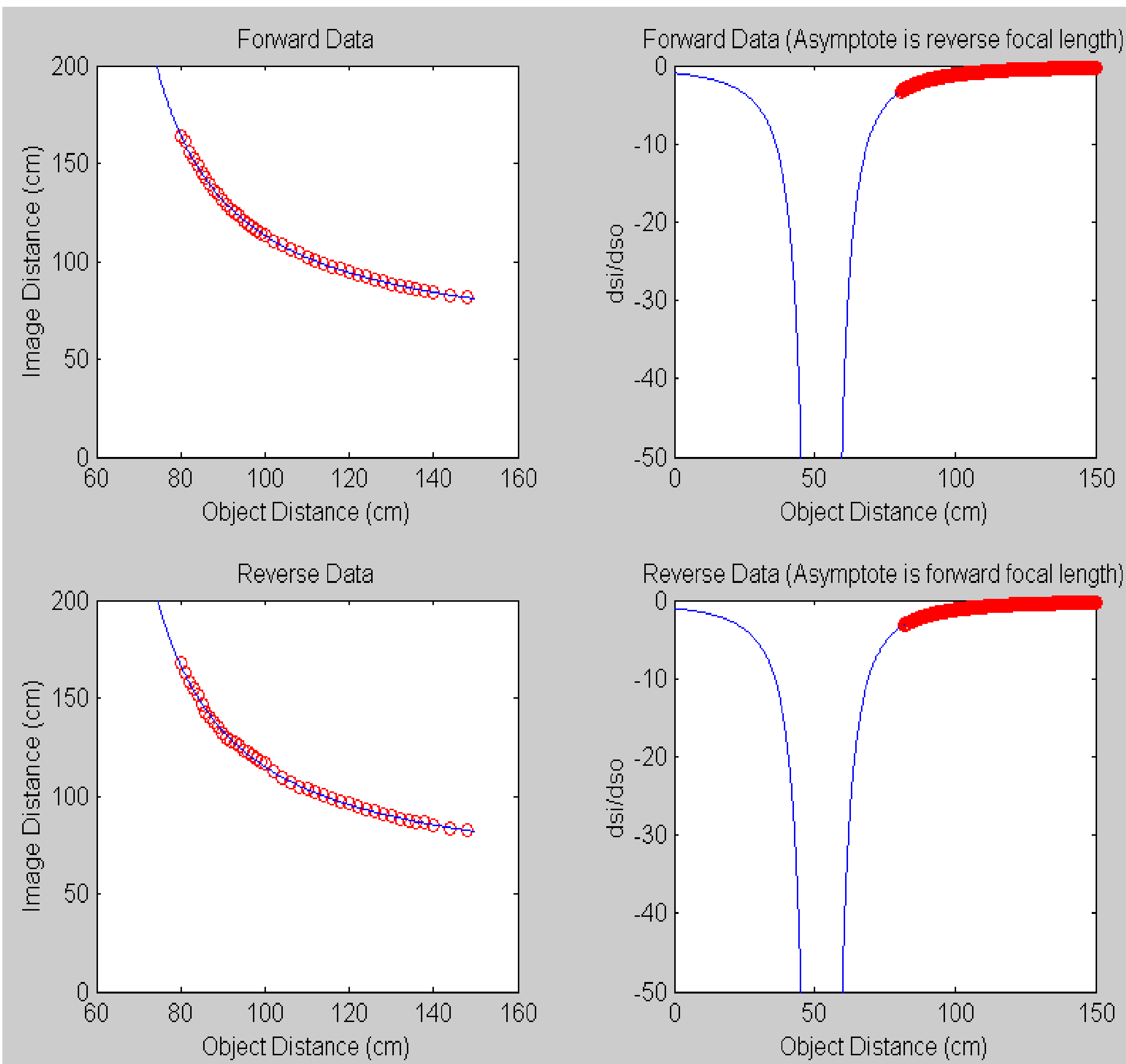

Figure 15. Plots of s_i vs. s_o and ds_i/ds_o vs. s_o for the camera objective at 334 nm.

4. 370 nm Wavelength

Data taken using the 370 nm bandpass filter resulted in focal lengths from the principal planes of 51.9 and 55.2 cm, a forward focal length of 55.1 cm, and a reverse focal length of 57.0 cm. The system lens matrix was:

$$M_{\text{Camera-370}} = \begin{pmatrix} 1.0281 & -5.0892 \\ -0.0187 & 1.0651 \end{pmatrix}.$$

Plots of image distance vs. object distance and ds_i/ds_o vs. object distance including the fitted curve are shown in Figure 16.

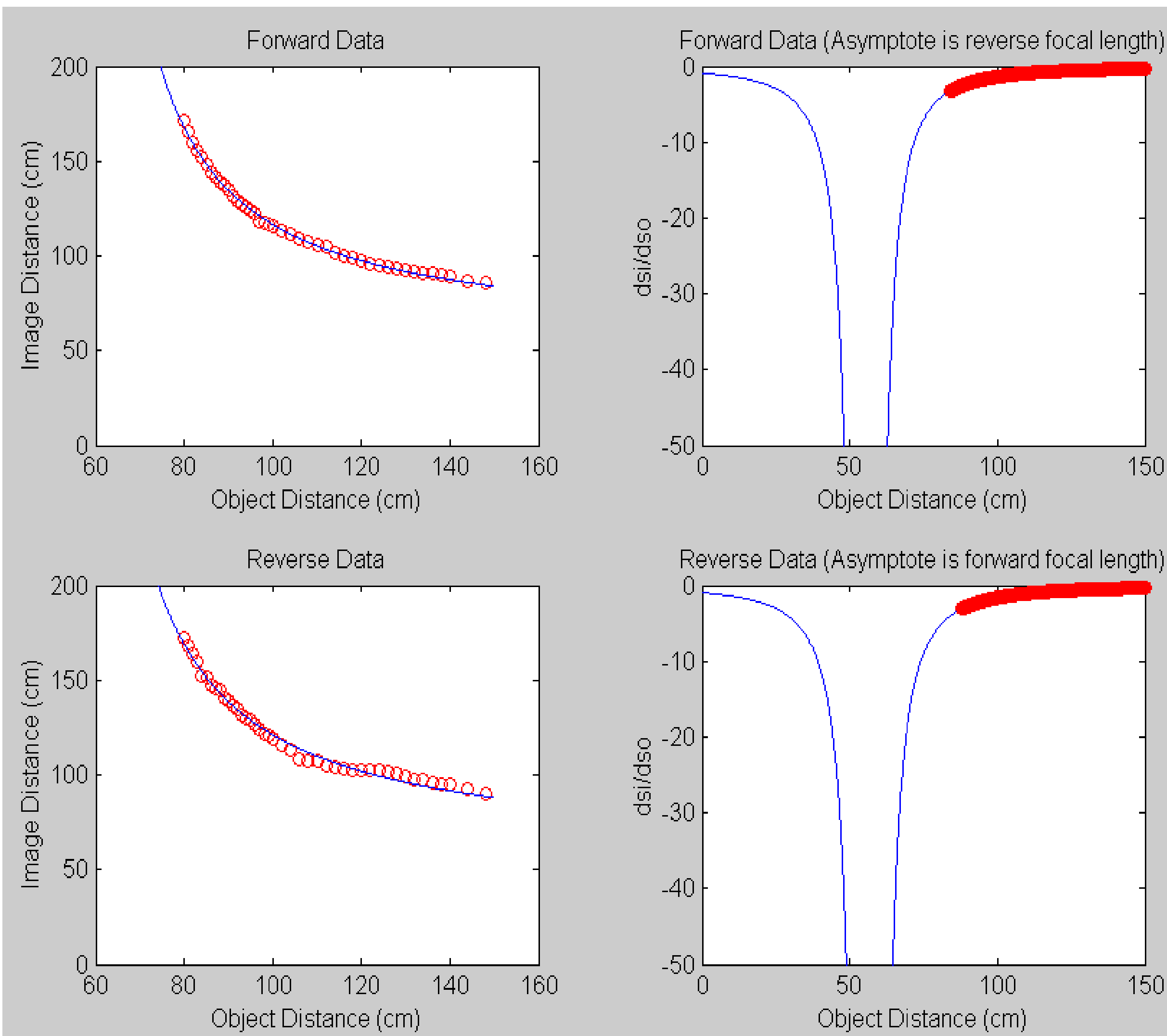

Figure 16. Plots of s_i vs. s_o and ds_i/ds_o vs. s_o for the camera objective at 370 nm.

E. ERROR ANALYSIS

Typically, error bars are used when plotting data against a curve or function that has been fitted to that data. In this case the error bars were not plotted because they were approximately the same size as the circles represent the data points themselves. Measurements collected using the camera objective are naturally larger due to the longer focal length of that lens and the fact that a bending mirror had to be used in order to perform the experiment. As the number of measurements increases due to an increased number of components in the optical path the errors associated with each measurement compound. The error associated with each individual measurement of s_i was ½ of one gradation of the measuring device used. Since that measurement was made in one step for the primary objective, that number is the error associated with those measurements. However, the camera objective required image distances longer than the measuring device being used. In order to accomplish this, an optical mounting base was attached to the optical table at a constant distance from the base of the camera and s_i was measured from this point, effectively doubling the number of measurements required to determine s_i. The error (δ) associated with these values of s_i was determined using the following standard equation:

$$\delta_{total} = \sqrt{\delta_1^2 + \delta_2^2} \ .$$

Finally, as the filter wavelengths approached those of visible light the image grew less sharp when focused. This is not unexpected, as the lens systems were designed to have minimal aberrations at UV wavelengths, with optimum performance at λ~300 nm. Errors associated with image and object distance measurements are given in the table below.

Lens System and Filter	**δs_i**	**δs_o**
Primary Objective (220 nm)	+/- 0.5 mm	+/- 1 mm
Primary Objective (300 nm)	+/- 0.5 mm	+/- 1 mm
Primary Objective (334 nm)	+/- 0.5 mm	+/- 1 mm
Primary Objective (370 nm)	+/- 0.5 mm	+/- 2 mm

Camera Objective (220 nm)	+/- 0.71 mm	+/- 2 mm
Camera Objective (300 nm)	+/- 0.71 mm	+/- 2 mm
Camera Objective (334 nm)	+/- 0.71 mm	+/- 2 mm
Camera Objective (370 nm)	+/- 0.71 mm	+/- 3 mm

Table 3. Image and object distance measurement errors.

Recall that the confidence level in the results of the analysis is directly related to the focal lengths as measured from the principal planes. These focal lengths should, in theory, be exactly equal in magnitude and as the difference in their magnitudes grows, in reality, the level of confidence in the results decreases proportionally. The results given earlier show a high level of confidence in the 300 and 334 nm results from both lens systems and a much lower level confidence in the 220 and 370 nm results. The fact that the same trend is seen from both lens systems indicates that these less reliable results are somehow linked to the filters and does not stem from the method, measurement techniques, lens systems, or other apparatus used to generate the data.

For the purposes of this analysis the uncertainty associated with the forward and reverse focal lengths as measured from the barrel is assumed to be equal to the difference in magnitudes of the calculated focal lengths as measured from the principal planes. The forward and reverse focal lengths and their associated uncertainties are given in Tables 4 and 5.

Wavelength	Forward Focal Length	Reverse Focal Length	Uncertainty
220 nm	18.9 cm	31.5 cm	+/- 3.1 cm
300 nm	23.4 cm	25.7 cm	+/- 0.2 cm
334 nm	24.1 cm	25.1 cm	+/- 0.5 cm
370 nm	21.4 cm	35.9 cm	+/- 3.3 cm

Table 4. Results summary for the primary objective.

Wavelength	Forward Focal Length	Reverse Focal Length	Uncertainty
220 nm	58.8 cm	41.8 cm	+/- 4.9 cm
300 nm	53.0 cm	51.6 cm	+/- 0.3 cm
334 nm	52.0 cm	52.9 cm	+/- 0.5 cm
370 nm	55.1 cm	57.0 cm	+/- 1.7 cm

Table 5. Results summary for the camera objective.

V. CONCLUSION

A. FINAL RESULTS

The primary goal of this thesis experiment was to quantify the chromatic aberration characteristics of the LINUS lens systems. Due to the lack of reliable results from the 220 and 370 nm filters these results are less accurate than originally hoped. The following figures were generated by using a simple spreadsheet; they show the basic trend of chromatic effects on focal length for the primary and camera objective lenses.

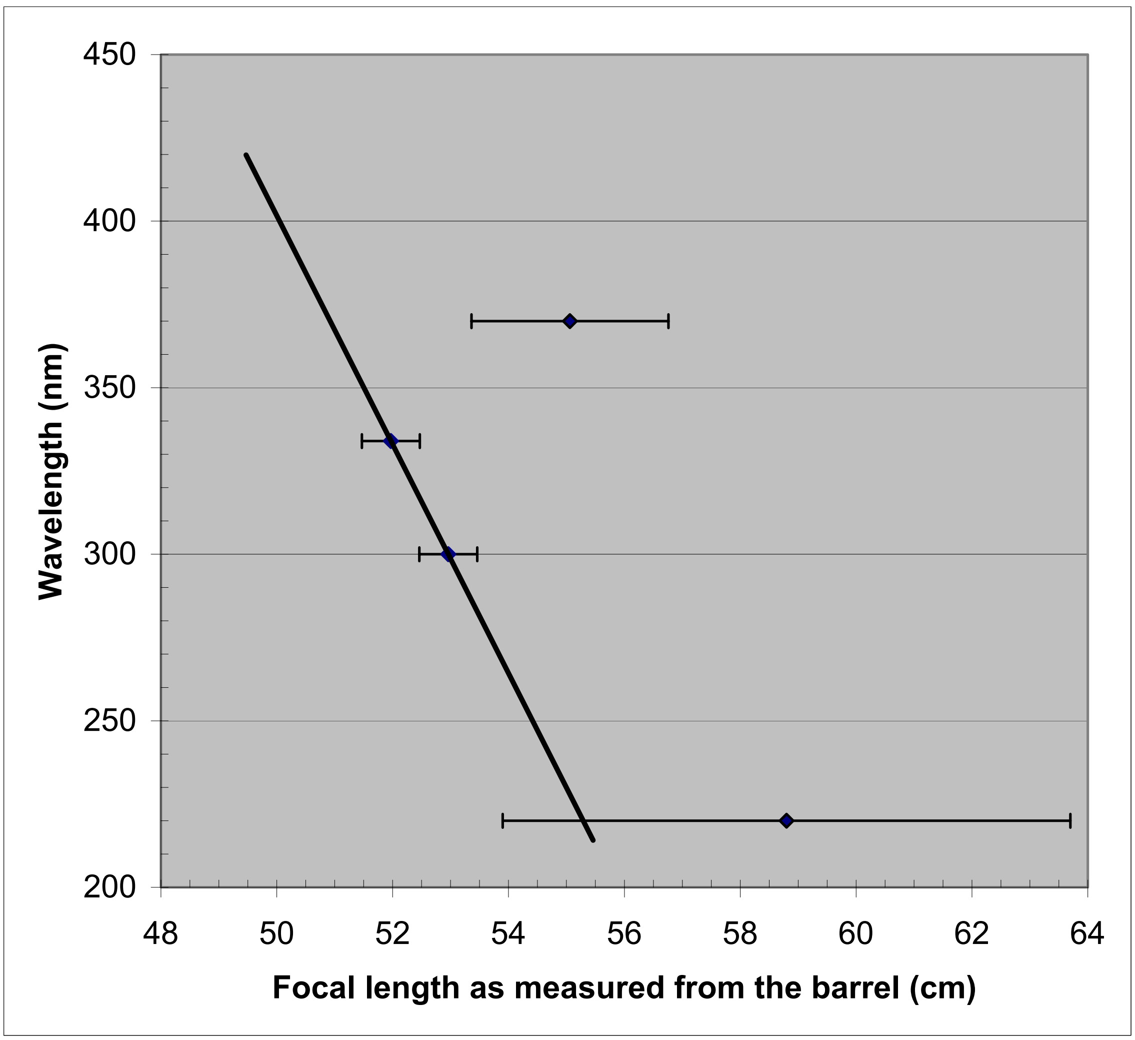

Figure 17. Chromatic aberration characteristics of LINUS' camera objective.

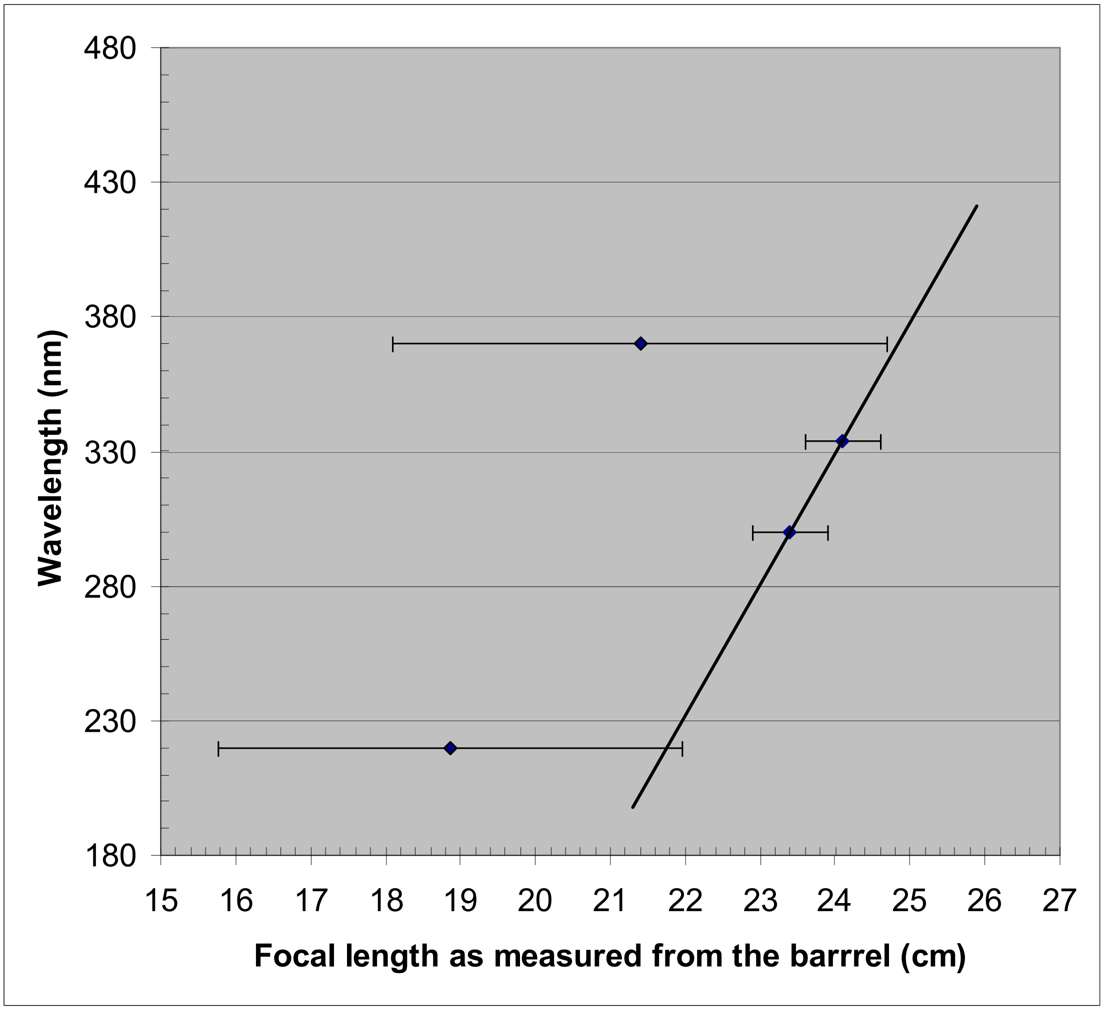

Figure 18. Chromatic aberration characteristics of LINUS' primary objective.

B. RECOMMENDATIONS

Obviously the linear interpolation of two data points is unambiguous, but should be interpreted with caution. It is, however the only option available at this time. This problem cannot be corrected until the nature of the problems with the 220 and 370 nm filters is understood. It is recommended that the cause of errors in the 220 and 370 nm filter data be explored and determined. Once the nature of these errors is understood a second set of measurements should be made and analyzed. This will allow for a more accurate characterization of the chromatic aberration for these lenses.

APPENDIX A. EXPERIMENTAL DATA

Data from the Primary Objective at 220 nm													
Forward							Reverse						
s_i	s_o^f	s_o	Δs_o	Δs_i	Avg s_o	$\Delta s_i/\Delta s_o$	s_i	s_o^r	s_o	Δs_o	Δs_i	Avg s_o	$\Delta s_i/\Delta s_o$
40	69.4	77.582	n/a	n/a	n/a	n/a	40	58.6	65.375	n/a	n/a	n/a	n/a
41	56.3	64.482	-13.1	1	71.032	-0.07634	41	56.1	62.875	-2.5	1	64.125	-0.4
42	53.4	61.582	-2.9	1	63.032	-0.34483	42	53.4	60.175	-2.7	1	61.525	-0.37037
43	49.9	58.082	-3.5	1	59.832	-0.28571	43	50.9	57.675	-2.5	1	58.925	-0.4
44	47.9	56.082	-2	1	57.082	-0.5	44	48.2	54.975	-2.7	1	56.325	-0.37037
45	46.7	54.882	-1.2	1	55.482	-0.83333	45	45.9	52.675	-2.3	1	53.825	-0.43478
46	45.2	53.382	-1.5	1	54.132	-0.66667	46	44.2	50.975	-1.7	1	51.825	-0.58824
47	43.9	52.082	-1.3	1	52.732	-0.76923	47	43.1	49.875	-1.1	1	50.425	-0.90909
48	41.2	49.382	-2.7	1	50.732	-0.37037	48	41.7	48.475	-1.4	1	49.175	-0.71429
49	40.4	48.582	-0.8	1	48.982	-1.25	49	41.1	47.875	-0.6	1	48.175	-1.66667
50	39.2	47.382	-1.2	1	47.982	-0.83333	50	40.2	46.975	-0.9	1	47.425	-1.11111
51	38.9	47.082	-0.3	1	47.232	-3.33333	51	39.4	46.175	-0.8	1	46.575	-1.25
52	38.2	46.382	-0.7	1	46.732	-1.42857	52	38.5	45.275	-0.9	1	45.725	-1.11111
54	37	45.182	-1.2	2	45.782	-1.66667	54	37.1	43.875	-1.4	2	44.575	-1.42857
56	36.3	44.482	-0.7	2	44.832	-2.85714	56	36	42.775	-1.1	2	43.325	-1.81818
58	35.1	43.282	-1.2	2	43.882	-1.66667	58	34.9	41.675	-1.1	2	42.225	-1.81818
60	33.7	41.882	-1.4	2	42.582	-1.42857	60	33.7	40.475	-1.2	2	41.075	-1.66667
62	32.4	40.582	-1.3	2	41.232	-1.53846	62	32.4	39.175	-1.3	2	39.825	-1.53846
64	31.1	39.282	-1.3	2	39.932	-1.53846	64	31.3	38.075	-1.1	2	38.625	-1.81818
66	30.5	38.682	-0.6	2	38.982	-3.33333	66	30	36.775	-1.3	2	37.425	-1.53846
69	29.2	37.382	-1.3	3	38.032	-2.30769	69	28.9	35.675	-1.1	3	36.225	-2.72727
72	28.1	36.282	-1.1	3	36.832	-2.72727	72	27.6	34.375	-1.3	3	35.025	-2.30769
75	27.1	35.282	-1	3	35.782	-3	75	26.9	33.675	-0.7	3	34.025	-4.28571
78	26.5	34.682	-0.6	3	34.982	-5	78	26.1	32.875	-0.8	3	33.275	-3.75
82	25.6	33.782	-0.9	4	34.232	-4.44444	82	25.3	32.075	-0.8	4	32.475	-5
86	25.3	33.482	-0.3	4	33.632	-13.3333	86	24.9	31.675	-0.4	4	31.875	-10
90	24.7	32.882	-0.6	4	33.182	-6.66667	90	24.7	31.475	-0.2	4	31.575	-20

Data from the Primary Objective at 300 nm													
Forward							*Reverse*						
s_i	s^f_o	s_o	Δs_o	Δs_i	Avg s_o	$\Delta s_i/\Delta s_o$	s_i	s^r_o	s_o	Δs_o	Δs_i	Avg s_o	$\Delta s_i/\Delta s_o$
40	73.9	82.082	n/a	n/a	n/a	n/a	40	75.8	82.575	n/a	n/a	n/a	n/a
41	69.5	77.682	-4.4	1	79.882	-0.22727	41	71	77.775	-4.8	1	80.175	-0.20833
42	64.8	72.982	-4.7	1	75.332	-0.21277	42	67.9	74.675	-3.1	1	76.225	-0.32258
43	63.3	71.482	-1.5	1	72.232	-0.66667	43	64	70.775	-3.9	1	72.725	-0.25641
44	59.6	67.782	-3.7	1	69.632	-0.27027	44	60.8	67.575	-3.2	1	69.175	-0.3125
45	57.6	65.782	-2	1	66.782	-0.5	45	58.4	65.175	-2.4	1	66.375	-0.41667
46	55.1	63.282	-2.5	1	64.532	-0.4	46	56.1	62.875	-2.3	1	64.025	-0.43478
47	53.2	61.382	-1.9	1	62.332	-0.52632	47	53.6	60.375	-2.5	1	61.625	-0.4
48	51.2	59.382	-2	1	60.382	-0.5	48	51.7	58.475	-1.9	1	59.425	-0.52632
49	49.9	58.082	-1.3	1	58.732	-0.76923	49	50.1	56.875	-1.6	1	57.675	-0.625
50	48.6	56.782	-1.3	1	57.432	-0.76923	50	48.4	55.175	-1.7	1	56.025	-0.58824
51	47.1	55.282	-1.5	1	56.032	-0.66667	51	47.3	54.075	-1.1	1	54.625	-0.90909
52	45.2	53.382	-1.9	1	54.332	-0.52632	52	46.2	52.975	-1.1	1	53.525	-0.90909
53	44.5	52.682	-0.7	1	53.032	-1.42857	53	44.8	51.575	-1.4	1	52.275	-0.71429
54	43.9	52.082	-0.6	1	52.382	-1.66667	54	43.7	50.475	-1.1	1	51.025	-0.90909
55	42.7	50.882	-1.2	1	51.482	-0.83333	55	42.8	49.575	-0.9	1	50.025	-1.11111
56	41.8	49.982	-0.9	1	50.432	-1.11111	56	41.9	48.675	-0.9	1	49.125	-1.11111
57	41.2	49.382	-0.6	1	49.682	-1.66667	57	41.1	47.875	-0.8	1	48.275	-1.25
58	40.3	48.482	-0.9	1	48.932	-1.11111	58	40.7	47.475	-0.4	1	47.675	-2.5
60	38.7	46.882	-1.6	2	47.682	-1.25	60	38.8	45.575	-1.9	2	46.525	-1.05263
62	37.8	45.982	-0.9	2	46.432	-2.22222	62	37.5	44.275	-1.3	2	44.925	-1.53846
64	36.4	44.582	-1.4	2	45.282	-1.42857	64	36.1	42.875	-1.4	2	43.575	-1.42857
66	35.4	43.582	-1	2	44.082	-2	66	35.1	41.875	-1	2	42.375	-2
68	34.8	42.982	-0.6	2	43.282	-3.33333	68	34.4	41.175	-0.7	2	41.525	-2.85714
70	33.7	41.882	-1.1	2	42.432	-1.81818	70	33.6	40.375	-0.8	2	40.775	-2.5
72	33	41.182	-0.7	2	41.532	-2.85714	72	32.8	39.575	-0.8	2	39.975	-2.5
74	32.2	40.382	-0.8	2	40.782	-2.5	74	32.2	38.975	-0.6	2	39.275	-3.33333
76	31.5	39.682	-0.7	2	40.032	-2.85714	76	31.4	38.175	-0.8	2	38.575	-2.5
79	30.9	39.082	-0.6	3	39.382	-5	79	30.6	37.375	-0.8	3	37.775	-3.75
82	30	38.182	-0.9	3	38.632	-3.33333	82	29.9	36.675	-0.7	3	37.025	-4.28571
86	29.2	37.382	-0.8	4	37.782	-5	86	29	35.775	-0.9	4	36.225	-4.44444
90	28.5	36.682	-0.7	4	37.032	-5.71429	90	28.2	34.975	-0.8	4	35.375	-5

Data from the Primary Objective at 334 nm													
Forward							*Reverse*						
s_i	s^f_o	s_o	Δs_o	Δs_i	Avg s_o	$\Delta s_i/\Delta s_o$	s_i	s^r_o	s_o	Δs_o	Δs_i	Avg s_o	$\Delta s_i/\Delta s_o$
40	78.4	86.582	n/a	n/a	n/a	n/a	40	82	88.775	n/a	n/a	n/a	n/a
41	74.8	82.982	-3.6	1	84.782	-0.27778	41	76	82.775	-6	1	85.775	-0.16667
42	71.1	79.282	-3.7	1	81.132	-0.27027	42	71.4	78.175	-4.6	1	80.475	-0.21739
43	67.2	75.382	-3.9	1	77.332	-0.25641	43	67.2	73.975	-4.2	1	76.075	-0.2381
44	64	72.182	-3.2	1	73.782	-0.3125	44	64	70.775	-3.2	1	72.375	-0.3125
45	61.2	69.382	-2.8	1	70.782	-0.35714	45	61.1	67.875	-2.9	1	69.325	-0.34483
46	59	67.182	-2.2	1	68.282	-0.45455	46	58.9	65.675	-2.2	1	66.775	-0.45455
47	56.3	64.482	-2.7	1	65.832	-0.37037	47	56.5	63.275	-2.4	1	64.475	-0.41667
48	53.9	62.082	-2.4	1	63.282	-0.41667	48	54	60.775	-2.5	1	62.025	-0.4
49	52.5	60.682	-1.4	1	61.382	-0.71429	49	52.1	58.875	-1.9	1	59.825	-0.52632
50	50.8	58.982	-1.7	1	59.832	-0.58824	50	50.8	57.575	-1.3	1	58.225	-0.76923
51	48.9	57.082	-1.9	1	58.032	-0.52632	51	49.2	55.975	-1.6	1	56.775	-0.625
52	48	56.182	-0.9	1	56.632	-1.11111	52	47.9	54.675	-1.3	1	55.325	-0.76923
53	46.8	54.982	-1.2	1	55.582	-0.83333	53	46.6	53.375	-1.3	1	54.025	-0.76923
54	45.2	53.382	-1.6	1	54.182	-0.625	54	45.5	52.275	-1.1	1	52.825	-0.90909
55	44.5	52.682	-0.7	1	53.032	-1.42857	55	44.2	50.975	-1.3	1	51.625	-0.76923
56	43.8	51.982	-0.7	1	52.332	-1.42857	56	43.5	50.275	-0.7	1	50.625	-1.42857
57	42.3	50.482	-1.5	1	51.232	-0.66667	57	42.6	49.375	-0.9	1	49.825	-1.11111
58	41.7	49.882	-0.6	1	50.182	-1.66667	58	41.6	48.375	-1	1	48.875	-1
60	40.1	48.282	-1.6	2	49.082	-1.25	60	40.1	46.875	-1.5	2	47.625	-1.33333
62	38.8	46.982	-1.3	2	47.632	-1.53846	62	38.8	45.575	-1.3	2	46.225	-1.53846
64	37.7	45.882	-1.1	2	46.432	-1.81818	64	37.7	44.475	-1.1	2	45.025	-1.81818
66	36.6	44.782	-1.1	2	45.332	-1.81818	66	36.6	43.375	-1.1	2	43.925	-1.81818
68	35.8	43.982	-0.8	2	44.382	-2.5	68	35.8	42.575	-0.8	2	42.975	-2.5
70	34.9	43.082	-0.9	2	43.532	-2.22222	70	34.5	41.275	-1.3	2	41.925	-1.53846
72	33.9	42.082	-1	2	42.582	-2	72	34	40.775	-0.5	2	41.025	-4
74	33.3	41.482	-0.6	2	41.782	-3.33333	74	33.3	40.075	-0.7	2	40.425	-2.85714
76	32.7	40.882	-0.6	2	41.182	-3.33333	76	32.6	39.375	-0.7	2	39.725	-2.85714
79	31.9	40.082	-0.8	3	40.482	-3.75	79	31.6	38.375	-1	3	38.875	-3
82	31	39.182	-0.9	3	39.632	-3.33333	82	30.8	37.575	-0.8	3	37.975	-3.75
86	29.9	38.082	-1.1	4	38.632	-3.63636	86	29.9	36.675	-0.9	4	37.125	-4.44444
90	29.2	37.382	-0.7	4	37.732	-5.71429	90	29	35.775	-0.9	4	36.225	-4.44444

Data from the Primary Objective at 370 nm													
Forward							Reverse						
s_i	s^f_o	s_o	Δs_o	Δs_i	Avg s_o	$\Delta s_i/\Delta s_o$	s_i	s^r_o	s_o	Δs_o	Δs_i	Avg s_o	$\Delta s_i/\Delta s_o$
40	81.8	89.982	n/a	n/a	n/a	n/a	40	84.2	90.975	n/a	n/a	n/a	n/a
41	75.2	83.382	-6.6	1	86.682	-0.15152	41	78.8	85.575	-5.4	1	88.275	-0.18519
42	72.2	80.382	-3	1	81.882	-0.33333	42	75.5	82.275	-3.3	1	83.925	-0.30303
43	67	75.182	-5.2	1	77.782	-0.19231	43	71.7	78.475	-3.8	1	80.375	-0.26316
44	62.1	70.282	-4.9	1	72.732	-0.20408	44	66.5	73.275	-5.2	1	75.875	-0.19231
45	59.3	67.482	-2.8	1	68.882	-0.35714	45	62.5	69.275	-4	1	71.275	-0.25
46	55.3	63.482	-4	1	65.482	-0.25	46	59.7	66.475	-2.8	1	67.875	-0.35714
47	53.4	61.582	-1.9	1	62.532	-0.52632	47	57.9	64.675	-1.8	1	65.575	-0.55556
48	51.5	59.682	-1.9	1	60.632	-0.52632	48	55.9	62.675	-2	1	63.675	-0.5
49	49.3	57.482	-2.2	1	58.582	-0.45455	49	53.5	60.275	-2.4	1	61.475	-0.41667
50	47.8	55.982	-1.5	1	56.732	-0.66667	50	51.8	58.575	-1.7	1	59.425	-0.58824
51	47	55.182	-0.8	1	55.582	-1.25	51	50.4	57.175	-1.4	1	57.875	-0.71429
52	46	54.182	-1	1	54.682	-1	52	48.8	55.575	-1.6	1	56.375	-0.625
53	44.9	53.082	-1.1	1	53.632	-0.90909	53	47.6	54.375	-1.2	1	54.975	-0.83333
54	44.2	52.382	-0.7	1	52.732	-1.42857	54	46.3	53.075	-1.3	1	53.725	-0.76923
55	42.8	50.982	-1.4	1	51.682	-0.71429	55	45.3	52.075	-1	1	52.575	-1
56	42	50.182	-0.8	1	50.582	-1.25	56	44.7	51.475	-0.6	1	51.775	-1.66667
57	41.4	49.582	-0.6	1	49.882	-1.66667	57	43.9	50.675	-0.8	1	51.075	-1.25
58	40.6	48.782	-0.8	1	49.182	-1.25	58	43	49.775	-0.9	1	50.225	-1.11111
59	40	48.182	-0.6	1	48.482	-1.66667	60	41.2	47.975	-1.8	2	48.875	-1.11111
60	39.4	47.582	-0.6	1	47.882	-1.66667	62	40.1	46.875	-1.1	2	47.425	-1.81818
61	38.6	46.782	-0.8	1	47.182	-1.25	64	38.4	45.175	-1.7	2	46.025	-1.17647
62	37.9	46.082	-0.7	1	46.432	-1.42857	66	37.1	43.875	-1.3	2	44.525	-1.53846
63	37.2	45.382	-0.7	1	45.732	-1.42857	68	36.4	43.175	-0.7	2	43.525	-2.85714
69	36	44.182	-1.2	6	44.782	-5	70	35.4	42.175	-1	2	42.675	-2
71	35.2	43.382	-0.8	2	43.782	-2.5	72	34.5	41.275	-0.9	2	41.725	-2.22222
73	34.3	42.482	-0.9	2	42.932	-2.22222	74	33.7	40.475	-0.8	2	40.875	-2.5
75	33.6	41.782	-0.7	2	42.132	-2.85714	76	33.1	39.875	-0.6	2	40.175	-3.33333
77	32.8	40.982	-0.8	2	41.382	-2.5	79	32	38.775	-1.1	3	39.325	-2.72727
80	32	40.182	-0.8	3	40.582	-3.75	82	31.3	38.075	-0.7	3	38.425	-4.28571
83	31.3	39.482	-0.7	3	39.832	-4.28571	86	30.3	37.075	-1	4	37.575	-4
86	30.5	38.682	-0.8	3	39.082	-3.75	90	29.4	36.175	-0.9	4	36.625	-4.44444

Data from the Camera Objective at 220 nm															
Forward								Reverse							
s_i	d_{nm}	s'_o	s_o	Δs_o	Δs_i	Avg s_o	$\Delta s_i/\Delta s_o$	s_i	d_{nm}	s'_o	s_o	Δs_o	Δs_i	Avg s_o	$\Delta s_i/\Delta s_o$
80	44.2	120.9	127.784	n/a	n/a	n/a	n/a	80	44.5	121.2	129.257	n/a	n/a	n/a	n/a
81	41.1	116.8	123.684	-4.1	1	125.734	-0.2439024	81	43	118.7	126.757	-2.5	1	128.007	-0.4
82	40.5	115.2	122.084	-1.6	1	122.884	-0.625	82	40.4	115.1	123.157	-3.6	1	124.957	-0.2777778
83	38.4	112.1	118.984	-3.1	1	120.534	-0.3225806	83	39.7	113.4	121.457	-1.7	1	122.307	-0.5882353
84	36.9	109.6	116.484	-2.5	1	117.734	-0.4	84	38	110.7	118.757	-2.7	1	120.107	-0.3703704
85	36.2	107.9	114.784	-1.7	1	115.634	-0.5882353	85	36.6	108.3	116.357	-2.4	1	117.557	-0.4166667
86	35	105.7	112.584	-2.2	1	113.684	-0.4545455	86	36.7	107.4	115.457	-0.9	1	115.907	-1.1111111
87	34.4	104.1	110.984	-1.6	1	111.784	-0.625	87	34	103.7	111.757	-3.7	1	113.607	-0.2702703
88	34.2	102.9	109.784	-1.2	1	110.384	-0.8333333	88	32.9	101.6	109.657	-2.1	1	110.707	-0.4761905
89	33.8	101.5	108.384	-1.4	1	109.084	-0.7142857	89	31.9	99.6	107.657	-2	1	108.657	-0.5
90	32.4	99.1	105.984	-2.4	1	107.184	-0.4166667	90	30	96.7	104.757	-2.9	1	106.207	-0.3448276
91	31.8	97.5	104.384	-1.6	1	105.184	-0.625	91	29.1	94.8	102.857	-1.9	1	103.807	-0.5263158
92	31.8	96.5	103.384	-1	1	103.884	-1	92	28.9	93.6	101.657	-1.2	1	102.257	-0.8333333
93	31.8	95.5	102.384	-1	1	102.884	-1	93	28.3	92	100.057	-1.6	1	100.857	-0.625
94	31.9	94.6	101.484	-0.9	1	101.934	-1.1111111	94	28.1	90.8	98.857	-1.2	1	99.457	-0.8333333
95	31.6	93.3	100.184	-1.3	1	100.834	-0.7692308	95	27.8	89.5	97.557	-1.3	1	98.207	-0.7692308
96	31.2	91.9	98.784	-1.4	1	99.484	-0.7142857	96	27.6	88.3	96.357	-1.2	1	96.957	-0.8333333
97	31	90.7	97.584	-1.2	1	98.184	-0.8333333	97	27.3	87	95.057	-1.3	1	95.707	-0.7692308
98	30.3	89	95.884	-1.7	1	96.734	-0.5882353	98	27.2	85.9	93.957	-1.1	1	94.507	-0.9090909
99	30.2	87.9	94.784	-1.1	1	95.334	-0.9090909	99	28.4	86.1	94.157	0.2	1	94.057	5
100	29.6	86.3	93.184	-1.6	1	93.984	-0.625	100	29.1	85.8	93.857	-0.3	1	94.007	-3.3333333
102	31.1	85.8	92.684	-0.5	2	92.934	-4	102	28.4	83.1	91.157	-2.7	2	92.507	-0.7407407
104	31.8	84.5	91.384	-1.3	2	92.034	-1.5384615	104	29.3	82	90.057	-1.1	2	90.607	-1.8181818
106	32	82.7	89.584	-1.8	2	90.484	-1.1111111	106	30	80.7	88.757	-1.3	2	89.407	-1.5384615
108	31.8	80.5	87.384	-2.2	2	88.484	-0.9090909	108	31.9	80.6	88.657	-0.1	2	88.707	-20
110	31.9	78.6	85.484	-1.9	2	86.434	-1.0526316	110	31.1	77.8	85.857	-2.8	2	87.257	-0.7142857
112	32.2	76.9	83.784	-1.7	2	84.634	-1.1764706	112	32.2	76.9	84.957	-0.9	2	85.407	-2.2222222
114	32.3	75	81.884	-1.9	2	82.834	-1.0526316	114	32.7	75.4	83.457	-1.5	2	84.207	-1.3333333
116	32.8	73.5	80.384	-1.5	2	81.134	-1.3333333	116	35.4	76.1	84.157	0.7	2	83.807	2.85714286
118	35.6	74.3	81.184	0.8	2	80.784	2.5	118	36.2	74.9	82.957	-1.2	2	83.557	-1.6666667
120	37	73.7	80.584	-0.6	2	80.884	-3.3333333	120	36.5	73.2	81.257	-1.7	2	82.107	-1.1764706
122	37.9	72.6	79.484	-1.1	2	80.034	-1.8181818	122	37.1	71.8	79.857	-1.4	2	80.557	-1.4285714
124	38.5	71.2	78.084	-1.4	2	78.784	-1.4285714	124	38.2	70.9	78.957	-0.9	2	79.407	-2.2222222
126	39.6	70.3	77.184	-0.9	2	77.634	-2.2222222	126	39.3	70	78.057	-0.9	2	78.507	-2.2222222
128	41.1	69.8	76.684	-0.5	2	76.934	-4	128	40.4	69.1	77.157	-0.9	2	77.607	-2.2222222
130	42.6	69.3	76.184	-0.5	2	76.434	-4	130	41.9	68.6	76.657	-0.5	2	76.907	-4
132	44.1	68.8	75.684	-0.5	2	75.934	-4	132	43	67.7	75.757	-0.9	2	76.207	-2.2222222
134	44.9	67.6	74.484	-1.2	2	75.084	-1.6666667	134	44.4	67.1	75.157	-0.6	2	75.457	-3.3333333
136	46.1	66.8	73.684	-0.8	2	74.084	-2.5	136	45.9	66.6	74.657	-0.5	2	74.907	-4
138	47.6	66.3	73.184	-0.5	2	73.434	-4	138	47.3	66	74.057	-0.6	2	74.357	-3.3333333
140	48.9	65.6	72.484	-0.7	2	72.834	-2.8571429	140	49.1	65.8	73.857	-0.2	2	73.957	-10
144	52.2	64.9	71.784	-0.7	4	72.134	-5.7142857	144	51.9	64.6	72.657	-1.2	4	73.257	-3.3333333
148	55	63.7	70.584	-1.2	4	71.184	-3.3333333	148	55.2	63.9	71.957	-0.7	4	72.307	-5.7142857

Data from the Camera Objective at 300 nm															
Forward								Reverse							
s_i	d_{nm}	s'_o	s_o	Δs_o	Δs_i	Avg s_o	$\Delta s_i/\Delta s_o$	s_i	d_{nm}	s'_o	s_o	Δs_o	Δs_i	Avg s_o	$\Delta s_i/\Delta s_o$
80	72.2	148.9	155.784	n/a	n/a	n/a	n/a	80	74.9	151.6	159.657	n/a	n/a	n/a	n/a
81	69.4	145.1	151.984	-3.8	1	153.884	-0.2631579	81	71.8	147.5	155.557	-4.1	1	157.607	-0.2439024
82	66	140.7	147.584	-4.4	1	149.784	-0.2272727	82	68.3	143	151.057	-4.5	1	153.307	-0.2222222
83	63.9	137.6	144.484	-3.1	1	146.034	-0.3225806	83	64.8	138.5	146.557	-4.5	1	148.807	-0.2222222
84	61.2	133.9	140.784	-3.7	1	142.634	-0.2702703	84	63.7	136.4	144.457	-2.1	1	145.507	-0.4761905
85	60	131.7	138.584	-2.2	1	139.684	-0.4545455	85	61.1	132.8	140.857	-3.6	1	142.657	-0.2777778
86	57.9	128.6	135.484	-3.1	1	137.034	-0.3225806	86	59.8	130.5	138.557	-2.3	1	139.707	-0.4347826
87	55.9	125.6	132.484	-3	1	133.984	-0.3333333	87	57.7	127.4	135.457	-3.1	1	137.007	-0.3225806
88	54.6	123.3	130.184	-2.3	1	131.334	-0.4347826	88	56.6	125.3	133.357	-2.1	1	134.407	-0.4761905
89	53.1	120.8	127.684	-2.5	1	128.934	-0.4	89	54.7	122.4	130.457	-2.9	1	131.907	-0.3448276
90	51.6	118.3	125.184	-2.5	1	126.434	-0.4	90	53	119.7	127.757	-2.7	1	129.107	-0.3703704
91	51.4	117.1	123.984	-1.2	1	124.584	-0.8333333	91	51	116.7	124.757	-3	1	126.257	-0.3333333
92	50.1	114.8	121.684	-2.3	1	122.834	-0.4347826	92	50.2	114.9	122.957	-1.8	1	123.857	-0.5555556
93	49.2	112.9	119.784	-1.9	1	120.734	-0.5263158	93	49.5	113.2	121.257	-1.7	1	122.107	-0.5882353
94	48.3	111	117.884	-1.9	1	118.834	-0.5263158	94	48.2	110.9	118.957	-2.3	1	120.107	-0.4347826
95	47.5	109.2	116.084	-1.8	1	116.984	-0.5555556	95	47.6	109.3	117.357	-1.6	1	118.157	-0.625
96	47.1	107.8	114.684	-1.4	1	115.384	-0.7142857	96	47.2	107.9	115.957	-1.4	1	116.657	-0.7142857
97	47.2	106.9	113.784	-0.9	1	114.234	-1.1111111	97	47.3	107	115.057	-0.9	1	115.507	-1.1111111
98	46.8	105.5	112.384	-1.4	1	113.084	-0.7142857	98	46.8	105.5	113.557	-1.5	1	114.307	-0.6666667
99	46.2	103.9	110.784	-1.6	1	111.584	-0.625	99	46.5	104.2	112.257	-1.3	1	112.907	-0.7692308
100	45.5	102.2	109.084	-1.7	1	109.934	-0.5882353	100	46.3	103	111.057	-1.2	1	111.657	-0.8333333
102	45.4	100.1	106.984	-2.1	2	108.034	-0.952381	102	45.8	100.5	108.557	-2.5	2	109.807	-0.8
104	45.2	97.9	104.784	-2.2	2	105.884	-0.9090909	104	45.5	98.2	106.257	-2.3	2	107.407	-0.8695652
106	45	95.7	102.584	-2.2	2	103.684	-0.9090909	106	44.8	95.5	103.557	-2.7	2	104.907	-0.7407407
108	45.2	93.9	100.784	-1.8	2	101.684	-1.1111111	108	44.9	93.6	101.657	-1.9	2	102.607	-1.0526316
110	45.9	92.6	99.484	-1.3	2	100.134	-1.5384615	110	44.4	91.1	99.157	-2.5	2	100.407	-0.8
112	45.4	90.1	96.984	-2.5	2	98.234	-0.8	112	45.7	90.4	98.457	-0.7	2	98.807	-2.8571429
114	45.9	88.6	95.484	-1.5	2	96.234	-1.3333333	114	45.9	88.6	96.657	-1.8	2	97.557	-1.1111111
116	46.7	87.4	94.284	-1.2	2	94.884	-1.6666667	116	46	86.7	94.757	-1.9	2	95.707	-1.0526316
118	47.1	85.8	92.684	-1.6	2	93.484	-1.25	118	46.8	85.5	93.557	-1.2	2	94.157	-1.6666667
120	47.6	84.3	91.184	-1.5	2	91.934	-1.3333333	120	47.8	84.5	92.557	-1	2	93.057	-2
122	49	83.7	90.584	-0.6	2	90.884	-3.3333333	122	48.7	83.4	91.457	-1.1	2	92.007	-1.8181818
124	50.4	83.1	89.984	-0.6	2	90.284	-3.3333333	124	49.4	82.1	90.157	-1.3	2	90.807	-1.5384615
126	51.1	81.8	88.684	-1.3	2	89.334	-1.5384615	126	50.1	80.8	88.857	-1.3	2	89.507	-1.5384615
128	52.1	80.8	87.684	-1	2	88.184	-2	128	51.4	80.1	88.157	-0.7	2	88.507	-2.8571429
130	52.8	79.5	86.384	-1.3	2	87.034	-1.5384615	130	52.3	79	87.057	-1.1	2	87.607	-1.8181818
132	53.7	78.4	85.284	-1.1	2	85.834	-1.8181818	132	53	77.7	85.757	-1.3	2	86.407	-1.5384615
134	54.9	77.6	84.484	-0.8	2	84.884	-2.5	134	54.4	77.1	85.157	-0.6	2	85.457	-3.3333333
136	56.2	76.9	83.784	-0.7	2	84.134	-2.8571429	136	55.4	76.1	84.157	-1	2	84.657	-2
138	57.4	76.1	82.984	-0.8	2	83.384	-2.5	138	56.6	75.3	83.357	-0.8	2	83.757	-2.5
140	58.5	75.2	82.084	-0.9	2	82.534	-2.2222222	140	57.8	74.5	82.557	-0.8	2	82.957	-2.5
144	60.8	73.5	80.384	-1.7	4	81.234	-2.3529412	144	61	73.7	81.757	-0.8	4	82.157	-5
148	63.9	72.6	79.484	-0.9	4	79.934	-4.4444444	148	63.2	71.9	79.957	-1.8	4	80.857	-2.2222222

Data from the Camera Objective at 334 nm

Forward								*Reverse*							
s_i	d_{nm}	s'_o	s_o	Δs_o	Δs_i	Avg s_o	$\Delta s_i/\Delta s_o$	s_i	d_{nm}	s'_o	s_o	Δs_o	Δs_i	Avg s_o	$\Delta s_i/\Delta s_o$
80	80.2	156.9	163.784	n/a	n/a	n/a	n/a	80	83	159.7	167.757	n/a	n/a	n/a	n/a
81	78.6	154.3	161.184	-2.6	1	162.484	-0.3846154	81	79	154.7	162.757	-5	1	165.257	-0.2
82	74.3	149	155.884	-5.3	1	158.534	-0.1886792	82	75.1	149.8	157.857	-4.9	1	160.307	-0.2040816
83	71.5	145.2	152.084	-3.8	1	153.984	-0.2631579	83	73.2	146.9	154.957	-2.9	1	156.407	-0.3448276
84	69.4	142.1	148.984	-3.1	1	150.534	-0.3225806	84	70.7	143.4	151.457	-3.5	1	153.207	-0.2857143
85	66.6	138.3	145.184	-3.8	1	147.084	-0.2631579	85	67.1	138.8	146.857	-4.6	1	149.157	-0.2173913
86	65	135.7	142.584	-2.6	1	143.884	-0.3846154	86	64.1	134.8	142.857	-4	1	144.857	-0.25
87	62.5	132.2	139.084	-3.5	1	140.834	-0.2857143	87	62.4	132.1	140.157	-2.7	1	141.507	-0.3703704
88	60.9	129.6	136.484	-2.6	1	137.784	-0.3846154	88	61	129.7	137.757	-2.4	1	138.957	-0.4166667
89	59.9	127.6	134.484	-2	1	135.484	-0.5	89	59.3	127	135.057	-2.7	1	136.407	-0.3703704
90	57.9	124.6	131.484	-3	1	132.984	-0.3333333	90	57.4	124.1	132.157	-2.9	1	133.607	-0.3448276
91	56.1	121.8	128.684	-2.8	1	130.084	-0.3571429	91	56.2	121.9	129.957	-2.2	1	131.057	-0.4545455
92	54.7	119.4	126.284	-2.4	1	127.484	-0.4166667	92	55.4	120.1	128.157	-1.8	1	129.057	-0.5555556
93	54	117.7	124.584	-1.7	1	125.434	-0.5882353	93	55.5	119.2	127.257	-0.9	1	127.707	-1.1111111
94	53.2	115.9	122.784	-1.8	1	123.684	-0.5555556	94	54.8	117.5	125.557	-1.7	1	126.407	-0.5882353
95	52.3	114	120.884	-1.9	1	121.834	-0.5263158	95	53.6	115.3	123.357	-2.2	1	124.457	-0.4545455
96	51.6	112.3	119.184	-1.7	1	120.034	-0.5882353	96	53.3	114	122.057	-1.3	1	122.707	-0.7692308
97	51.3	111	117.884	-1.3	1	118.534	-0.7692308	97	52.9	112.6	120.657	-1.4	1	121.357	-0.7142857
98	50.5	109.2	116.084	-1.8	1	116.984	-0.5555556	98	52.1	110.8	118.857	-1.8	1	119.757	-0.5555556
99	49.8	107.5	114.384	-1.7	1	115.234	-0.5882353	99	51.9	109.6	117.657	-1.2	1	118.257	-0.8333333
100	49.5	106.2	113.084	-1.3	1	113.734	-0.7692308	100	51.7	108.4	116.457	-1.2	1	117.057	-0.8333333
102	48.8	103.5	110.384	-2.7	2	111.734	-0.7407407	102	49.9	104.6	112.657	-3.8	2	114.557	-0.5263158
104	48.6	101.3	108.184	-2.2	2	109.284	-0.9090909	104	48.9	101.6	109.657	-3	2	111.157	-0.6666667
106	48.2	98.9	105.784	-2.4	2	106.984	-0.8333333	106	48.2	98.9	106.957	-2.7	2	108.307	-0.7407407
108	49	97.7	104.584	-1.2	2	105.184	-1.6666667	108	47.8	96.5	104.557	-2.4	2	105.757	-0.8333333
110	48.7	95.4	102.284	-2.3	2	103.434	-0.8695652	110	48.7	95.4	103.457	-1.1	2	104.007	-1.8181818
112	49	93.7	100.584	-1.7	2	101.434	-1.1764706	112	49	93.7	101.757	-1.7	2	102.607	-1.1764706
114	49.2	91.9	98.784	-1.8	2	99.684	-1.1111111	114	49.4	92.1	100.157	-1.6	2	100.957	-1.25
116	49.9	90.6	97.484	-1.3	2	98.134	-1.5384615	116	50	90.7	98.757	-1.4	2	99.457	-1.4285714
118	50.6	89.3	96.184	-1.3	2	96.834	-1.5384615	118	50.7	89.4	97.457	-1.3	2	98.107	-1.5384615
120	51.4	88.1	94.984	-1.2	2	95.584	-1.6666667	120	51.2	87.9	95.957	-1.5	2	96.707	-1.3333333
122	51.9	86.6	93.484	-1.5	2	94.234	-1.3333333	122	51.9	86.6	94.657	-1.3	2	95.307	-1.5384615
124	52.6	85.3	92.184	-1.3	2	92.834	-1.5384615	124	52.6	85.3	93.357	-1.3	2	94.007	-1.5384615
126	53.3	84	90.884	-1.3	2	91.534	-1.5384615	126	53.3	84	92.057	-1.3	2	92.707	-1.5384615
128	54	82.7	89.584	-1.3	2	90.234	-1.5384615	128	54.1	82.8	90.857	-1.2	2	91.457	-1.6666667
130	54.8	81.5	88.384	-1.2	2	88.984	-1.6666667	130	54.7	81.4	89.457	-1.4	2	90.157	-1.4285714
132	55.9	80.6	87.484	-0.9	2	87.934	-2.2222222	132	55.4	80.1	88.157	-1.3	2	88.807	-1.5384615
134	56.8	79.5	86.384	-1.1	2	86.934	-1.8181818	134	56.9	79.6	87.657	-0.5	2	87.907	-4
136	58	78.7	85.584	-0.8	2	85.984	-2.5	136	57.9	78.6	86.657	-1	2	87.157	-2
138	59.1	77.8	84.684	-0.9	2	85.134	-2.2222222	138	59.5	78.2	86.257	-0.4	2	86.457	-5
140	60.2	76.9	83.784	-0.9	2	84.234	-2.2222222	140	60.4	77.1	85.157	-1.1	2	85.707	-1.8181818
144	63.3	76	82.884	-0.9	4	83.334	-4.4444444	144	62.6	75.3	83.357	-1.8	4	84.257	-2.2222222
148	65.8	74.5	81.384	-1.5	4	82.134	-2.6666667	148	65.4	74.1	82.157	-1.2	4	82.757	-3.3333333

Data from the Camera Objective at 370 nm

Forward								Reverse							
s_i	d_{nm}	s'_o	s_o	Δs_o	Δs_i	Avg s_o	$\Delta s_i/\Delta s_o$	s_i	d_{nm}	s'_o	s_o	Δs_o	Δs_i	Avg s_o	$\Delta s_i/\Delta s_o$
80	88.2	164.9	171.784	n/a	n/a	n/a	n/a	80	87.4	164.1	172.157	n/a	n/a	n/a	n/a
81	82.7	158.4	165.284	-6.5	1	168.534	-0.1538462	81	84	159.7	167.757	-4.4	1	169.957	-0.2272727
82	78.1	152.8	159.684	-5.6	1	162.484	-0.1785714	82	80.8	155.5	163.557	-4.2	1	165.657	-0.2380952
83	75.4	149.1	155.984	-3.7	1	157.834	-0.2702703	83	77.6	151.3	159.357	-4.2	1	161.457	-0.2380952
84	72.9	145.6	152.484	-3.5	1	154.234	-0.2857143	84	71.7	144.4	152.457	-6.9	1	155.907	-0.1449275
85	69.5	141.2	148.084	-4.4	1	150.284	-0.2272727	85	71.5	143.2	151.257	-1.2	1	151.857	-0.8333333
86	66.4	137.1	143.984	-4.1	1	146.034	-0.2439024	86	68.8	139.5	147.557	-3.7	1	149.407	-0.2702703
87	64.5	134.2	141.084	-2.9	1	142.534	-0.3448276	87	68.3	138	146.057	-1.5	1	146.807	-0.6666667
88	63.6	132.3	139.184	-1.9	1	140.134	-0.5263158	88	68	136.7	144.757	-1.3	1	145.407	-0.7692308
89	62.6	130.3	137.184	-2	1	138.184	-0.5	89	64.8	132.5	140.557	-4.2	1	142.657	-0.2380952
90	61.3	128	134.884	-2.3	1	136.034	-0.4347826	90	64	130.7	138.757	-1.8	1	139.657	-0.5555556
91	58.6	124.3	131.184	-3.7	1	133.034	-0.2702703	91	62.4	128.1	136.157	-2.6	1	137.457	-0.3846154
92	57.6	122.3	129.184	-2	1	130.184	-0.5	92	61.7	126.4	134.457	-1.7	1	135.307	-0.5882353
93	56.4	120.1	126.984	-2.2	1	128.084	-0.4545455	93	60.1	123.8	131.857	-2.6	1	133.157	-0.3846154
94	55.8	118.5	125.384	-1.6	1	126.184	-0.625	94	59.5	122.2	130.257	-1.6	1	131.057	-0.625
95	55.1	116.8	123.684	-1.7	1	124.534	-0.5882353	95	59.1	120.8	128.857	-1.4	1	129.557	-0.7142857
96	55	115.7	122.584	-1.1	1	123.134	-0.9090909	96	58.2	118.9	126.957	-1.9	1	127.907	-0.5263158
97	51.8	111.5	118.384	-4.2	1	120.484	-0.2380952	97	56.6	116.3	124.357	-2.6	1	125.657	-0.3846154
98	51.6	110.3	117.184	-1.2	1	117.784	-0.8333333	98	55.2	113.9	121.957	-2.4	1	123.157	-0.4166667
99	51.9	109.6	116.484	-0.7	1	116.834	-1.4285714	99	55.3	113	121.057	-0.9	1	121.507	-1.1111111
100	52.4	109.1	115.984	-0.5	1	116.234	-2	100	54	110.7	118.757	-2.3	1	119.907	-0.4347826
102	51.7	106.4	113.284	-2.7	2	114.634	-0.7407407	102	53.1	107.8	115.857	-2.9	2	117.307	-0.6896552
104	51.8	104.5	111.384	-1.9	2	112.334	-1.0526316	104	52.5	105.2	113.257	-2.6	2	114.557	-0.7692308
106	51.9	102.6	109.484	-1.9	2	110.434	-1.0526316	106	49.2	99.9	107.957	-5.3	2	110.607	-0.3773585
108	51.8	100.5	107.384	-2.1	2	108.434	-0.952381	108	51	99.7	107.757	-0.2	2	107.857	-10
110	52.4	99.1	105.984	-1.4	2	106.684	-1.4285714	110	52.4	99.1	107.157	-0.6	2	107.457	-3.3333333
112	53	97.7	104.584	-1.4	2	105.284	-1.4285714	112	52.2	96.9	104.957	-2.2	2	106.057	-0.9090909
114	51.9	94.6	101.484	-3.1	2	103.034	-0.6451613	114	53.2	95.9	103.957	-1	2	104.457	-2
116	52.6	93.3	100.184	-1.3	2	100.834	-1.5384615	116	54.2	94.9	102.957	-1	2	103.457	-2
118	53.2	91.9	98.784	-1.4	2	99.484	-1.4285714	118	55.8	94.5	102.557	-0.4	2	102.757	-5
120	54	90.7	97.584	-1.2	2	98.184	-1.6666667	120	57.6	94.3	102.357	-0.2	2	102.457	-10
122	54.6	89.3	96.184	-1.4	2	96.884	-1.4285714	122	59.5	94.2	102.257	-0.1	2	102.307	-20
124	55.5	88.2	95.084	-1.1	2	95.634	-1.8181818	124	61.4	94.1	102.157	-0.1	2	102.207	-20
126	56.4	87.1	93.984	-1.1	2	94.534	-1.8181818	126	63	93.7	101.757	-0.4	2	101.957	-5
128	57.8	86.5	93.384	-0.6	2	93.684	-3.3333333	128	63.8	92.5	100.557	-1.2	2	101.157	-1.6666667
130	58.9	85.6	92.484	-0.9	2	92.934	-2.2222222	130	64.4	91.1	99.157	-1.4	2	99.857	-1.4285714
132	60.2	84.9	91.784	-0.7	2	92.134	-2.8571429	132	64.7	89.4	97.457	-1.7	2	98.307	-1.1764706
134	61.6	84.3	91.184	-0.6	2	91.484	-3.3333333	134	66.4	89.1	97.157	-0.3	2	97.307	-6.6666667
136	63	83.7	90.584	-0.6	2	90.884	-3.3333333	136	67.2	87.9	95.957	-1.2	2	96.557	-1.6666667
138	64.5	83.2	90.084	-0.5	2	90.334	-4	138	68.4	87.1	95.157	-0.8	2	95.557	-2.5
140	65.4	82.1	88.984	-1.1	2	89.534	-1.8181818	140	70.3	87	95.057	-0.1	2	95.107	-20
144	67.3	80	86.884	-2.1	4	87.934	-1.9047619	144	72.1	84.8	92.857	-2.2	4	93.957	-1.8181818
148	69.9	78.6	85.484	-1.4	4	86.184	-2.8571429	148	73	81.7	89.757	-3.1	4	91.307	-1.2903226

Red Filtered Data from a Complex Lens									*(All distances are given in cm)*								
Forward									*Reverse*								
s_o	Near s_i	Far s_i	Δs_o	Δs_{IN}	Δs_{IF}	Avg so	$\Delta s_{IN}/\Delta s_o$	$\Delta s_{IF}/\Delta s_o$	s_o	Near s_i	Far s_i	Δs_o	Δs_{IN}	Δs_{IF}	Avg so	$\Delta s_{IN}/\Delta s_o$	$\Delta s_{IF}/\Delta s_o$
25.5	14.65	15.7	n/a	n/a	n/a	n/a	n/a	n/a	26	13.75	14.2	n/a	n/a	n/a	n/a	n/a	n/a
25	14.8	16	-0.5	0.15	0.3	25.25	-0.3	-0.6	25.5	13.9	14.95	-0.5	0.15	0.75	25.75	-0.3	-1.5
24.5	14.9	16.1	-0.5	0.1	0.1	24.75	-0.2	-0.2	25	14.1	15.2	-0.5	0.2	0.25	25.25	-0.4	-0.5
24	15.1	16.35	-0.5	0.2	0.25	24.25	-0.4	-0.5	24.5	14.3	15.3	-0.5	0.2	0.1	24.75	-0.4	-0.2
23.5	15.4	16.6	-0.5	0.3	0.25	23.75	-0.6	-0.5	24	14.4	15.5	-0.5	0.1	0.2	24.25	-0.2	-0.4
23	15.55	16.85	-0.5	0.15	0.25	23.25	-0.3	-0.5	23.5	14.7	15.9	-0.5	0.3	0.4	23.75	-0.6	-0.8
22.5	15.8	17.1	-0.5	0.25	0.25	22.75	-0.5	-0.5	23	14.9	16.2	-0.5	0.2	0.3	23.25	-0.4	-0.6
22	16	17.45	-0.5	0.2	0.35	22.25	-0.4	-0.7	22.5	15.2	16.4	-0.5	0.3	0.2	22.75	-0.6	-0.4
21.5	16.25	17.6	-0.5	0.25	0.15	21.75	-0.5	-0.3	22	15.5	16.8	-0.5	0.3	0.4	22.25	-0.6	-0.8
21	16.55	17.9	-0.5	0.3	0.3	21.25	-0.6	-0.6	21.5	15.8	17.2	-0.5	0.3	0.4	21.75	-0.6	-0.8
20.5	16.8	18.25	-0.5	0.25	0.35	20.75	-0.5	-0.7	21	16.1	17.5	-0.5	0.3	0.3	21.25	-0.6	-0.6
20	17.1	18.55	-0.5	0.3	0.3	20.25	-0.6	-0.6	20.5	16.5	18	-0.5	0.4	0.5	20.75	-0.8	-1
19.5	17.5	19.05	-0.5	0.4	0.5	19.75	-0.8	-1	20	16.9	18.45	-0.5	0.4	0.45	20.25	-0.8	-0.9
19	17.8	19.45	-0.5	0.3	0.4	19.25	-0.6	-0.8	19.5	17.4	19.05	-0.5	0.5	0.6	19.75	-1	-1.2
18.5	18.2	19.95	-0.5	0.4	0.5	18.75	-0.8	-1	19	17.8	19.5	-0.5	0.4	0.45	19.25	-0.8	-0.9
18	18.8	20.5	-0.5	0.6	0.55	18.25	-1.2	-1.1	18.5	18.4	20.2	-0.5	0.6	0.7	18.75	-1.2	-1.4
17.5	19.3	21.1	-0.5	0.5	0.6	17.75	-1	-1.2	18	19	21	-0.5	0.6	0.8	18.25	-1.2	-1.6
17	19.8	21.7	-0.5	0.5	0.6	17.25	-1	-1.2	17.5	19.55	21.8	-0.5	0.55	0.8	17.75	-1.1	-1.6
16.5	20.5	22.4	-0.5	0.7	0.7	16.75	-1.4	-1.4	17	20.2	22.6	-0.5	0.65	0.8	17.25	-1.3	-1.6
16	21.2	23.45	-0.5	0.7	1.05	16.25	-1.4	-2.1	16.5	21.1	23.8	-0.5	0.9	1.2	16.75	-1.8	-2.4
15.5	22	24.2	-0.5	0.8	0.75	15.75	-1.6	-1.5	16	22	24.95	-0.5	0.9	1.15	16.25	-1.8	-2.3
15	22.9	25.3	-0.5	0.9	1.1	15.25	-1.8	-2.2	15.5	23.05	26.3	-0.5	1.05	1.35	15.75	-2.1	-2.7
14.5	23.9	26.7	-0.5	1	1.4	14.75	-2	-2.8	15	24.4	27.8	-0.5	1.35	1.5	15.25	-2.7	-3
14	25.1	27.9	-0.5	1.2	1.2	14.25	-2.4	-2.4	14.5	25.8	29.65	-0.5	1.4	1.85	14.75	-2.8	-3.7
13.5	26.75	29.6	-0.5	1.65	1.7	13.75	-3.3	-3.4	14	27.9	32.3	-0.5	2.1	2.65	14.25	-4.2	-5.3
13	28.5	31.5	-0.5	1.75	1.9	13.25	-3.5	-3.8	13.5	29.7	35	-0.5	1.8	2.7	13.75	-3.6	-5.4

Yellow Filtered Data from a Complex Lens																	
Forward									*Reverse*								
s_o	Near s_i	Far s_i	Δs_o	Δs_{iN}	Δs_{iF}	Avg so	$\Delta s_{iN}/\Delta s_o$	$\Delta s_{iF}/\Delta s_o$	s_o	Near s_i	Far s_i	Δs_o	Δs_{iN}	Δs_{iF}	Avg so	$\Delta s_{iN}/\Delta s_o$	$\Delta s_{iF}/\Delta s_o$
23	15.5	16.8	n/a	n/a	n/a	n/a	n/a	n/a	23	15	16.2	n/a	n/a	n/a	n/a	n/a	n/a
22.5	15.7	17.1	-0.5	0.2	0.3	22.75	-0.4	-0.6	22.5	15.15	16.4	-0.5	0.15	0.2	22.75	-0.3	-0.4
22	16	17.35	-0.5	0.3	0.25	22.25	-0.6	-0.5	22	15.4	16.8	-0.5	0.25	0.4	22.25	-0.5	-0.8
21.5	16.3	17.7	-0.5	0.3	0.35	21.75	-0.6	-0.7	21.5	15.8	17.2	-0.5	0.4	0.4	21.75	-0.8	-0.8
21	16.55	18	-0.5	0.25	0.3	21.25	-0.5	-0.6	21	16.15	17.6	-0.5	0.35	0.4	21.25	-0.7	-0.8
20.5	16.8	18.3	-0.5	0.25	0.3	20.75	-0.5	-0.6	20.5	16.45	17.95	-0.5	0.3	0.35	20.75	-0.6	-0.7
20	17.15	18.7	-0.5	0.35	0.4	20.25	-0.7	-0.8	20	16.8	18.4	-0.5	0.35	0.45	20.25	-0.7	-0.9
19.5	17.5	19.05	-0.5	0.35	0.35	19.75	-0.7	-0.7	19.5	17.3	18.95	-0.5	0.5	0.55	19.75	-1	-1.1
19	17.9	19.55	-0.5	0.4	0.5	19.25	-0.8	-1	19	17.75	20.55	-0.5	0.45	1.6	19.25	-0.9	-3.2
18.5	18.3	19.95	-0.5	0.4	0.4	18.75	-0.8	-0.8	18.5	18.3	20.1	-0.5	0.55	-0.45	18.75	-1.1	0.9
18	18.8	20.55	-0.5	0.5	0.6	18.25	-1	-1.2	18	18.8	21	-0.5	0.5	0.9	18.25	-1	-1.8
17.5	19.2	21.15	-0.5	0.4	0.6	17.75	-0.8	-1.2	17.5	19.5	21.7	-0.5	0.7	0.7	17.75	-1.4	-1.4
17	19.85	21.7	-0.5	0.65	0.55	17.25	-1.3	-1.1	17	20.1	22.6	-0.5	0.6	0.9	17.25	-1.2	-1.8
16.5	20.5	22.45	-0.5	0.65	0.75	16.75	-1.3	-1.5	16.5	21.05	23.6	-0.5	0.95	1	16.75	-1.9	-2
16	21.3	23.2	-0.5	0.8	0.75	16.25	-1.6	-1.5	16	22	24.75	-0.5	0.95	1.15	16.25	-1.9	-2.3
15.5	22	24.15	-0.5	0.7	0.95	15.75	-1.4	-1.9	15.5	23	26.15	-0.5	1	1.4	15.75	-2	-2.8
15	22.95	25.3	-0.5	0.95	1.15	15.25	-1.9	-2.3	15	24.2	27.6	-0.5	1.2	1.45	15.25	-2.4	-2.9
14.5	23.95	26.55	-0.5	1	1.25	14.75	-2	-2.5	14.5	25.8	29.65	-0.5	1.6	2.05	14.75	-3.2	-4.1
14	25.35	27.9	-0.5	1.4	1.35	14.25	-2.8	-2.7	14	27.45	32	-0.5	1.65	2.35	14.25	-3.3	-4.7
13.5	26.65	29.6	-0.5	1.3	1.7	13.75	-2.6	-3.4	13.5	29.6	35	-0.5	2.15	3	13.75	-4.3	-6
13	28.5	31.7	-0.5	1.85	2.1	13.25	-3.7	-4.2	13	32.25	38.8	-0.5	2.65	3.8	13.25	-5.3	-7.6

Green Filtered Data from a Complex Lens							(All distances are given in cm)										
Forward									Reverse								
s_o	Near s_i	Far s_i	Δs_o	Δs_{iN}	Δs_{iF}	Avg so	$\Delta s_{iN}/\Delta s_o$	$\Delta s_{iF}/\Delta s_o$	s_o	Near s_i	Far s_i	Δs_o	Δs_{iN}	Δs_{iF}	Avg so	$\Delta s_{iN}/\Delta s_o$	$\Delta s_{iF}/\Delta s_o$
23	15.5	16.8	n/a	n/a	n/a	n/a	n/a	n/a	23	15	16.1	n/a	n/a	n/a	n/a	n/a	n/a
22.5	15.75	17.05	-0.5	0.25	0.25	22.75	-0.5	-0.5	22.5	15.2	16.4	-0.5	0.2	0.3	22.75	-0.4	-0.6
22	15.95	17.25	-0.5	0.2	0.2	22.25	-0.4	-0.4	22	15.4	16.85	-0.5	0.2	0.45	22.25	-0.4	-0.9
21.5	16.2	17.6	-0.5	0.25	0.35	21.75	-0.5	-0.7	21.5	15.7	17.1	-0.5	0.3	0.25	21.75	-0.6	-0.5
21	16.5	17.9	-0.5	0.3	0.3	21.25	-0.6	-0.6	21	16.1	17.6	-0.5	0.4	0.5	21.25	-0.8	-1
20.5	16.8	18.2	-0.5	0.3	0.3	20.75	-0.6	-0.6	20.5	16.45	17.95	-0.5	0.35	0.35	20.75	-0.7	-0.7
20	17.1	18.6	-0.5	0.3	0.4	20.25	-0.6	-0.8	20	16.9	18.45	-0.5	0.45	0.5	20.25	-0.9	-1
19.5	17.5	19	-0.5	0.4	0.4	19.75	-0.8	-0.8	19.5	17.2	19	-0.5	0.3	0.55	19.75	-0.6	-1.1
19	17.8	19.5	-0.5	0.3	0.5	19.25	-0.6	-1	19	17.65	19.5	-0.5	0.45	0.5	19.25	-0.9	-1
18.5	18.1	19.85	-0.5	0.3	0.35	18.75	-0.6	-0.7	18.5	18.2	20.1	-0.5	0.55	0.6	18.75	-1.1	-1.2
18	18.7	20.5	-0.5	0.6	0.65	18.25	-1.2	-1.3	18	18.85	20.85	-0.5	0.65	0.75	18.25	-1.3	-1.5
17.5	19.2	21	-0.5	0.5	0.5	17.75	-1	-1	17.5	19.4	21.7	-0.5	0.55	0.85	17.75	-1.1	-1.7
17	19.75	21.75	-0.5	0.55	0.75	17.25	-1.1	-1.5	17	20.1	22.55	-0.5	0.7	0.85	17.25	-1.4	-1.7
16.5	20.35	22.5	-0.5	0.6	0.75	16.75	-1.2	-1.5	16.5	21	23.6	-0.5	0.9	1.05	16.75	-1.8	-2.1
16	21.1	23.3	-0.5	0.75	0.8	16.25	-1.5	-1.6	16	21.9	24.85	-0.5	0.9	1.25	16.25	-1.8	-2.5
15.5	22.05	24.2	-0.5	0.95	0.9	15.75	-1.9	-1.8	15.5	23	26	-0.5	1.1	1.15	15.75	-2.2	-2.3
15	22.85	25.3	-0.5	0.8	1.1	15.25	-1.6	-2.2	15	24.15	27.7	-0.5	1.15	1.7	15.25	-2.3	-3.4
14.5	23.85	26.5	-0.5	1	1.2	14.75	-2	-2.4	14.5	25.7	29.65	-0.5	1.55	1.95	14.75	-3.1	-3.9
14	25.1	27.6	-0.5	1.25	1.1	14.25	-2.5	-2.2	14	27.35	31.05	-0.5	1.65	1.4	14.25	-3.3	-2.8
13.5	26.55	29.1	-0.5	1.45	1.5	13.75	-2.9	-3	13.5	29.55	34.05	-0.5	2.2	3	13.75	-4.4	-6
13	28.4	31.3	-0.5	1.85	2.2	13.25	-3.7	-4.4	13	32.35	38.65	-0.5	2.8	4.6	13.25	-5.6	-9.2
12.5		33.75	-0.5	0	2.45	12.75	0	-4.9									
12		36.8	-0.5	0	3.05	12.25	0	-6.1									

Blue-Green Filtered Data from a Complex Lens											
Forward						*Reverse*					
s_o	Far s_i	Δs_o	Δs_{iF}	Avg so	$\Delta s_{iF}/\Delta s_o$	s_o	Far s_i	Δs_o	Δs_{iF}	Avg so	$\Delta s_{iF}/\Delta s_o$
21	17.8	n/a	n/a	n/a	n/a	22	16.75	n/a	n/a	n/a	n/a
20.5	18.1	-0.5	0.3	20.75	-0.6	21.5	17.2	-0.5	0.45	21.75	-0.9
20	18.45	-0.5	0.35	20.25	-0.7	21	17.5	-0.5	0.3	21.25	-0.6
19.5	18.95	-0.5	0.5	19.75	-1	20.5	17.9	-0.5	0.4	20.75	-0.8
19	19.3	-0.5	0.35	19.25	-0.7	20	18.4	-0.5	0.5	20.25	-1
18.5	19.8	-0.5	0.5	18.75	-1	19.5	18.95	-0.5	0.55	19.75	-1.1
18	20.35	-0.5	0.55	18.25	-1.1	19	19.5	-0.5	0.55	19.25	-1.1
17.5	20.9	-0.5	0.55	17.75	-1.1	18.5	20.1	-0.5	0.6	18.75	-1.2
17	21.5	-0.5	0.6	17.25	-1.2	18	20.8	-0.5	0.7	18.25	-1.4
16.5	22.1	-0.5	0.6	16.75	-1.2	17.5	21.6	-0.5	0.8	17.75	-1.6
16	23	-0.5	0.9	16.25	-1.8	17	22.5	-0.5	0.9	17.25	-1.8
15.5	24	-0.5	1	15.75	-2	16.5	23.6	-0.5	1.1	16.75	-2.2
15	25.1	-0.5	1.1	15.25	-2.2	16	24.8	-0.5	1.2	16.25	-2.4
14.5	26.2	-0.5	1.1	14.75	-2.2	15.5	25.95	-0.5	1.15	15.75	-2.3
14	27.55	-0.5	1.35	14.25	-2.7	15	27.8	-0.5	1.85	15.25	-3.7
13.5	29.2	-0.5	1.65	13.75	-3.3	14.5	29.85	-0.5	2.05	14.75	-4.1
13	31.15	-0.5	1.95	13.25	-3.9	14	32.15	-0.5	2.3	14.25	-4.6
12.5	33.5	-0.5	2.35	12.75	-4.7	13.5	35.1	-0.5	2.95	13.75	-5.9
12	36.4	-0.5	2.9	12.25	-5.8	13	38.9	-0.5	3.8	13.25	-7.6

THIS PAGE INTENTIONALLY LEFT BLANK

APPENDIX B. MATLAB CODE

```
%Calculation of matrix elements for the
%Primary Objective from data collected using
%a 10 nm bandpass filter at 220 nm

clear all

%This portion of the program will load
%the image and object distance measurements
%taken in the lab, fit them to a general
%hyperbolic function, and use that function
%to generate another set of data for further
%analysis

%Import the initial data
load Lens3_220nmdata.dat;

%Create vectors for analysis with the curve
%fitting function
fwdxdata =[[1 0 0 0]*Lens3_220nmdata'];
fwdydata =[[0 1 0 0]*Lens3_220nmdata'];
revxdata =[[0 0 1 0]*Lens3_220nmdata'];
revydata =[[0 0 0 1]*Lens3_220nmdata'];

options=optimset('MaxFunEvals',1e30,'maxiter',5000);

%Use f's for initial curve fit of forward data
f0=[1 1 1 1];
[f resnorm]=lsqcurvefit(@GenHyperbola,f0,fwdxdata,fwdydata);

%Use r's for initial curve fit of reverse data
r0=[1 1 1 1];
[r resnorm]=lsqcurvefit(@GenHyperbola,r0,revxdata,revydata);

%Generation of new image and object distance data
fwdsi=35:0.1:100;
fwdso=((f(1).*fwdsi+f(2))./(f(3).*fwdsi+f(4)));

revsi=35:0.1:100;
revso=((r(1).*revsi+r(2))./(r(3).*revsi+r(4)));

%Plot results for this section

subplot(2,2,1); plot(fwdxdata,fwdydata,'ro');
        title('Forward Data');
        xlabel('Object Distance (cm)');
        ylabel('Image Distance (cm)');
        hold;
        plot(fwdsi,fwdso,'b');
        ylim([0 150]);
subplot(2,2,3); plot(revxdata,revydata,'ro');
        title('Reverse Data');
```

```
            xlabel('Object Distance (cm)');
            ylabel('Image Distance (cm)');
            hold;
            plot(revsi,revso,'b');
            ylim([0 150]);

%Generation of new dsi/dso data
fwddsidso=(f(1).*f(4)-f(2).*f(3))./(f(3).*fwdso-f(1)).^2;
revdsidso=(r(1).*r(4)-r(2).*r(3))./(r(3).*revso-r(1)).^2;

%This portion of the program will utilize the data
%generated earlier to calculate the matrix elements
%of the complex lens system

%Use a's for forward data
a0=[1 1];
[a resnorm]=lsqcurvefit(@thindsidso2,a0,fwdso,fwddsidso)

%Use b's for reverse data
b0=[1 1];
[b resnorm]=lsqcurvefit(@thindsidso2,b0,revso,revdsidso)

%Calculate Lens Matrix Elements
mc=-1/((b(1)+a(1))/2);
md=mc*(-((a(1)+b(1))/2)-a(2));
ma=1-mc*b(2);
mb=(ma*md-1)/mc;

lensmatrix=[ma mb;mc md]

mp=md/mc;
mq=-ma/mc;

fwdfocallength=abs(mq)
revfocallength=abs(mp)

xdatum=0:0.1:90;
fwdydatum=(-(a(1).^2)./(xdatum-a(2)-a(1)).^2);
revydatum=(-(b(1).^2)./(xdatum-b(2)-b(1)).^2);
subplot(2,2,2); plot(xdatum,fwdydatum);
            ylim([-50,0]);
            title('Forward Data (Asymptote is reverse focal length)');
            xlabel('Object Distance (cm)');
            ylabel('dsi/dso');
            hold;
            plot(fwdso,fwddsidso,'ro');
            xlim([0,100]);
subplot(2,2,4); plot(xdatum,revydatum);
            ylim([-50,0]);
            title('Reverse Data (Asymptote is forward focal length)');
            xlabel('Object Distance (cm)');
            ylabel('dsi/dso');
            hold;
            plot(revso,revdsidso,'ro');
            xlim([0,100]);
```

```
%Calculation of matrix elements for the
%Primary Objective from data collected using
%a 10 nm bandpass filter at 300 nm

clear all

%This portion of the program will load
%the image and object distance measurements
%taken in the lab, fit them to a general
%hyperbolic function, and use that function
%to generate another set of data for further
%analysis

%Import the initial data

load Lens3_300nmdata.dat;

%Create vectors for analysis with the curve
%fitting function
fwdxdata =[[1 0 0 0]*Lens3_300nmdata'];
fwdydata =[[0 1 0 0]*Lens3_300nmdata'];
revxdata =[[0 0 1 0]*Lens3_300nmdata'];
revydata =[[0 0 0 1]*Lens3_300nmdata'];

options=optimset('MaxFunEvals',1e30,'maxiter',5000);

%Use f's for initial curve fit of forward data
f0=[1 1 1 1];
[f resnorm]=lsqcurvefit(@GenHyperbola,f0,fwdxdata,fwdydata);

%Use r's for initial curve fit of reverse data
r0=[1 1 1 1];
[r resnorm]=lsqcurvefit(@GenHyperbola,r0,revxdata,revydata);

%Generation of new image and object distance data

fwdsi=35:0.1:100;
fwdso=((f(1).*fwdsi+f(2))./(f(3).*fwdsi+f(4)));

revsi=35:0.1:100;
revso=((r(1).*revsi+r(2))./(r(3).*revsi+r(4)));

%Plot results for this section

subplot(2,2,1); plot(fwdxdata,fwdydata,'ro');
        title('Forward Data');
        xlabel('Object Distance (cm)');
        ylabel('Image Distance (cm)');
        hold;
        plot(fwdsi,fwdso,'b');
        ylim([0 150]);
subplot(2,2,3); plot(revxdata,revydata,'ro');
        title('Reverse Data');
        xlabel('Object Distance (cm)');
        ylabel('Image Distance (cm)');
```

```
        hold;
        plot(revsi,revso,'b');
        ylim([0 150]);

%Generation of new dsi/dso data

fwddsidso=(f(1).*f(4)-f(2).*f(3))./(f(3).*fwdso-f(1)).^2;
revdsidso=(r(1).*r(4)-r(2).*r(3))./(r(3).*revso-r(1)).^2;

%This portion of the program will utilize the data
%generated earlier to calculate the matrix elements
%of the complex lens system

%Use a's for forward data
a0=[1 1];
[a resnorm]=lsqcurvefit(@thindsidso2,a0,fwdso,fwddsidso)

%Use b's for reverse data
b0=[1 1];
[b resnorm]=lsqcurvefit(@thindsidso2,b0,revso,revdsidso)

%Calculate Lens Matrix Elements
mc=-1/((b(1)+a(1))/2);
md=mc*(-((a(1)+b(1))/2)-a(2));
ma=1-mc*b(2);
mb=(ma*md-1)/mc;

lensmatrix=[ma mb;mc md]

mp=md/mc;
mq=-ma/mc;

fwdfocallength=abs(mq)
revfocallength=abs(mp)

xdatum=0:0.1:90;
fwdydatum=(-(a(1).^2)./(xdatum-a(2)-a(1)).^2);
revydatum=(-(b(1).^2)./(xdatum-b(2)-b(1)).^2);
subplot(2,2,2); plot(xdatum,fwdydatum);
        ylim([-50,0]);
        title('Forward Data (Asymptote is reverse focal length)');
        xlabel('Object Distance (cm)');
        ylabel('dsi/dso');
        hold;
        plot(fwdso,fwddsidso,'ro');
        xlim([0,100]);
subplot(2,2,4); plot(xdatum,revydatum);
        ylim([-50,0]);
        title('Reverse Data (Asymptote is forward focal length)');
        xlabel('Object Distance (cm)');
        ylabel('dsi/dso');
        hold;
        plot(revso,revdsidso,'ro');
        xlim([0,100]);
```

```
%Calculation of matrix elements for the
%Primary Objective from data collected using
%a 10 nm bandpass filter at 334 nm

clear all

%This portion of the program will load
%the image and object distance measurements
%taken in the lab, fit them to a general
%hyperbolic function, and use that function
%to generate another set of data for further
%analysis

%Import the initial data

load Lens3_334nmdata.dat;

%Create vectors for analysis with the curve
%fitting function
fwdxdata =[[1 0 0 0]*Lens3_334nmdata'];
fwdydata =[[0 1 0 0]*Lens3_334nmdata'];
revxdata =[[0 0 1 0]*Lens3_334nmdata'];
revydata =[[0 0 0 1]*Lens3_334nmdata'];

options=optimset('MaxFunEvals',1e30,'maxiter',5000);

%Use f's for initial curve fit of forward data
f0=[1 1 1 1];
[f resnorm]=lsqcurvefit(@GenHyperbola,f0,fwdxdata,fwdydata);

%Use r's for initial curve fit of reverse data
r0=[1 1 1 1];
[r resnorm]=lsqcurvefit(@GenHyperbola,r0,revxdata,revydata);

%Generation of new image and object distance data

fwdsi=35:0.1:100;
fwdso=((f(1).*fwdsi+f(2))./(f(3).*fwdsi+f(4)));

revsi=35:0.1:100;
revso=((r(1).*revsi+r(2))./(r(3).*revsi+r(4)));

%Plot results for this section

subplot(2,2,1); plot(fwdxdata,fwdydata,'ro');
        title('Forward Data');
        xlabel('Object Distance (cm)');
        ylabel('Image Distance (cm)');
        hold;
        plot(fwdsi,fwdso,'b');
        ylim([0 150]);
subplot(2,2,3); plot(revxdata,revydata,'ro');
        title('Reverse Data');
        xlabel('Object Distance (cm)');
        ylabel('Image Distance (cm)');
```

```
        hold;
        plot(revsi,revso,'b');
        ylim([0 150]);

%Generation of new dsi/dso data

fwddsidso=(f(1).*f(4)-f(2).*f(3))./(f(3).*fwdso-f(1)).^2;
revdsidso=(r(1).*r(4)-r(2).*r(3))./(r(3).*revso-r(1)).^2;

%This portion of the program will utilize the data
%generated earlier to calculate the matrix elements
%of the complex lens system

%Use a's for forward data
a0=[1 1];
[a resnorm]=lsqcurvefit(@thindsidso2,a0,fwdso,fwddsidso)

%Use b's for reverse data
b0=[1 1];
[b resnorm]=lsqcurvefit(@thindsidso2,b0,revso,revdsidso)

%Calculate Lens Matrix Elements
mc=-1/((b(1)+a(1))/2);
md=mc*(-((a(1)+b(1))/2)-a(2));
ma=1-mc*b(2);
mb=(ma*md-1)/mc;

lensmatrix=[ma mb;mc md]

mp=md/mc;
mq=-ma/mc;

fwdfocallength=abs(mq)
revfocallength=abs(mp)

xdatum=0:0.1:90;
fwdydatum=(-(a(1).^2)./(xdatum-a(2)-a(1)).^2);
revydatum=(-(b(1).^2)./(xdatum-b(2)-b(1)).^2);
subplot(2,2,2); plot(xdatum,fwdydatum);
        ylim([-50,0]);
        title('Forward Data (Asymptote is reverse focal length)');
        xlabel('Object Distance (cm)');
        ylabel('dsi/dso');
        hold;
        plot(fwdso,fwddsidso,'ro');
        xlim([0,100]);
subplot(2,2,4); plot(xdatum,revydatum);
        ylim([-50,0]);
        title('Reverse Data (Asymptote is forward focal length)');
        xlabel('Object Distance (cm)');
        ylabel('dsi/dso');
        hold;
        plot(revso,revdsidso,'ro');
        xlim([0,100]);
```

```
%Calculation of matrix elements for the
%Primary Objective from data collected using
%a 10 nm bandpass filter at 370 nm

clear all

%This portion of the program will load
%the image and object distance measurements
%taken in the lab, fit them to a general
%hyperbolic function, and use that function
%to generate another set of data for further
%analysis

%Import the initial data

load Lens3_370nmdata.dat;

%Create vectors for analysis with the curve
%fitting function
fwdxdata =[[1 0 0 0]*Lens3_370nmdata'];
fwdydata =[[0 1 0 0]*Lens3_370nmdata'];
revxdata =[[0 0 1 0]*Lens3_370nmdata'];
revydata =[[0 0 0 1]*Lens3_370nmdata'];

options=optimset('MaxFunEvals',1e30,'maxiter',5000);

%Use f's for initial curve fit of forward data
f0=[1 1 1 1];
[f resnorm]=lsqcurvefit(@GenHyperbola,f0,fwdxdata,fwdydata);

%Use r's for initial curve fit of reverse data
r0=[1 1 1 1];
[r resnorm]=lsqcurvefit(@GenHyperbola,r0,revxdata,revydata);

%Generation of new image and object distance data

fwdsi=35:0.1:100;
fwdso=((f(1).*fwdsi+f(2))./(f(3).*fwdsi+f(4)));

revsi=35:0.1:100;
revso=((r(1).*revsi+r(2))./(r(3).*revsi+r(4)));

%Plot results for this section

subplot(2,2,1); plot(fwdxdata,fwdydata,'ro');
        title('Forward Data');
        xlabel('Object Distance (cm)');
        ylabel('Image Distance (cm)');
        hold;
        plot(fwdsi,fwdso,'b');
        ylim([0 150]);
subplot(2,2,3); plot(revxdata,revydata,'ro');
        title('Reverse Data');
        xlabel('Object Distance (cm)');
        ylabel('Image Distance (cm)');
```

```
		hold;
		plot(revsi,revso,'b');
		ylim([0 150]);

%Generation of new dsi/dso data

fwddsidso=(f(1).*f(4)-f(2).*f(3))./(f(3).*fwdso-f(1)).^2;
revdsidso=(r(1).*r(4)-r(2).*r(3))./(r(3).*revso-r(1)).^2;

%This portion of the program will utilize the data
%generated earlier to calculate the matrix elements
%of the complex lens system

%Use a's for forward data
a0=[1 1];
[a resnorm]=lsqcurvefit(@thindsidso2,a0,fwdso,fwddsidso)

%Use b's for reverse data
b0=[1 1];
[b resnorm]=lsqcurvefit(@thindsidso2,b0,revso,revdsidso)

%Calculate Lens Matrix Elements
mc=-1/((b(1)+a(1))/2);
md=mc*(-((a(1)+b(1))/2)-a(2));
ma=1-mc*b(2);
mb=(ma*md-1)/mc;

lensmatrix=[ma mb;mc md]

mp=md/mc;
mq=-ma/mc;

fwdfocallength=abs(mq)
revfocallength=abs(mp)

xdatum=0:0.1:90;
fwdydatum=(-(a(1).^2)./(xdatum-a(2)-a(1)).^2);
revydatum=(-(b(1).^2)./(xdatum-b(2)-b(1)).^2);
subplot(2,2,2); plot(xdatum,fwdydatum);
		ylim([-50,0]);
		title('Forward Data (Asymptote is reverse focal length)');
		xlabel('Object Distance (cm)');
		ylabel('dsi/dso');
		hold;
		plot(fwdso,fwddsidso,'ro');
		xlim([0,100]);
subplot(2,2,4); plot(xdatum,revydatum);
		ylim([-50,0]);
		title('Reverse Data (Asymptote is forward focal length)');
		xlabel('Object Distance (cm)');
		ylabel('dsi/dso');
		hold;
		plot(revso,revdsidso,'ro');
		xlim([0,100]);
```

```
%Calculation of matrix elements for the
%Camera Objective from data collected using
%a 10 nm bandpass filter at 220 nm

clear all

%This portion of the program will load
%the image and object distance measurements
%taken in the lab, fit them to a general
%hyperbolic function, and use that function
%to generate another set of data for further
%analysis

%Import the initial data

load Lens1_220nmdata.dat;

%Create vectors for analysis with the curve
%fitting function
fwdxdata =[[1 0 0 0]*Lens1_220nmdata'];
fwdydata =[[0 1 0 0]*Lens1_220nmdata'];
revxdata =[[0 0 1 0]*Lens1_220nmdata'];
revydata =[[0 0 0 1]*Lens1_220nmdata'];

options=optimset('MaxFunEvals',1e30,'maxiter',5000);

%Use f's for initial curve fit of forward data
f0=[1 1 1 1];
[f resnorm]=lsqcurvefit(@GenHyperbola,f0,fwdxdata,fwdydata);

%Use r's for initial curve fit of reverse data
r0=[1 1 1 1];
[r resnorm]=lsqcurvefit(@GenHyperbola,r0,revxdata,revydata);

%Generation of new image and object distance data

fwdsi=60:0.1:150;
fwdso=((f(1).*fwdsi+f(2))./(f(3).*fwdsi+f(4)));

revsi=60:0.1:150;
revso=((r(1).*revsi+r(2))./(r(3).*revsi+r(4)));

%Plot results for this section

subplot(2,2,1); plot(fwdxdata,fwdydata,'ro');
        title('Forward Data');
        xlabel('Object Distance (cm)');
        ylabel('Image Distance (cm)');
        hold;
        plot(fwdsi,fwdso,'b');
        ylim([0 200]);
subplot(2,2,3); plot(revxdata,revydata,'ro');
        title('Reverse Data');
        xlabel('Object Distance (cm)');
        ylabel('Image Distance (cm)');
```

```
        hold;
        plot(revsi,revso,'b');
        ylim([0 200]);

%Generation of new dsi/dso data

fwddsidso=(f(1).*f(4)-f(2).*f(3))./(f(3).*fwdso-f(1)).^2;
revdsidso=(r(1).*r(4)-r(2).*r(3))./(r(3).*revso-r(1)).^2;

%This portion of the program will utilize the data
%generated earlier to calculate the matrix elements
%of the complex lens system

%Use a's for forward data
a0=[1 1];
[a resnorm]=lsqcurvefit(@thindsidso2,a0,fwdso,fwddsidso)

%Use b's for reverse data
b0=[1 1];
[b resnorm]=lsqcurvefit(@thindsidso2,b0,revso,revdsidso)

%Calculate Lens Matrix Elements
mc=-1/((b(1)+a(1))/2);
md=mc*(-((a(1)+b(1))/2)-a(2));
ma=1-mc*b(2);
mb=(ma*md-1)/mc;

lensmatrix=[ma mb;mc md]

mp=md/mc;
mq=-ma/mc;

fwdfocallength=abs(mq)
revfocallength=abs(mp)

xdatum=0:0.1:90;
fwdydatum=(-(a(1).^2)./(xdatum-a(2)-a(1)).^2);
revydatum=(-(b(1).^2)./(xdatum-b(2)-b(1)).^2);
subplot(2,2,2); plot(xdatum,fwdydatum);
        ylim([-50,0]);
        title('Forward Data (Asymptote is reverse focal length)');
        xlabel('Object Distance (cm)');
        ylabel('dsi/dso');
        hold;
        plot(fwdso,fwddsidso,'ro');
        xlim([0,150]);
subplot(2,2,4); plot(xdatum,revydatum);
        ylim([-50,0]);
        title('Reverse Data (Asymptote is forward focal length)');
        xlabel('Object Distance (cm)');
        ylabel('dsi/dso');
        hold;
        plot(revso,revdsidso,'ro');
        xlim([0,150]);
```

```
%Calculation of matrix elements for the
%Camera Objective from data collected using
%a 10 nm bandpass filter at 300 nm

clear all

%This portion of the program will load
%the image and object distance measurements
%taken in the lab, fit them to a general
%hyperbolic function, and use that function
%to generate another set of data for further
%analysis

%Import the initial data

load Lens1_300nmdata.dat;

%Create vectors for analysis with the curve
%fitting function
fwdxdata =[[1 0 0 0]*Lens1_300nmdata'];
fwdydata =[[0 1 0 0]*Lens1_300nmdata'];
revxdata =[[0 0 1 0]*Lens1_300nmdata'];
revydata =[[0 0 0 1]*Lens1_300nmdata'];

options=optimset('MaxFunEvals',1e30,'maxiter',5000);

%Use f's for initial curve fit of forward data
f0=[1 1 1 1];
[f resnorm]=lsqcurvefit(@GenHyperbola,f0,fwdxdata,fwdydata);

%Use r's for initial curve fit of reverse data
r0=[1 1 1 1];
[r resnorm]=lsqcurvefit(@GenHyperbola,r0,revxdata,revydata);

%Generation of new image and object distance data

fwdsi=60:0.1:150;
fwdso=((f(1).*fwdsi+f(2))./(f(3).*fwdsi+f(4)));

revsi=60:0.1:150;
revso=((r(1).*revsi+r(2))./(r(3).*revsi+r(4)));

%Plot results for this section

subplot(2,2,1); plot(fwdxdata,fwdydata,'ro');
        title('Forward Data');
        xlabel('Object Distance (cm)');
        ylabel('Image Distance (cm)');
        hold;
        plot(fwdsi,fwdso,'b');
        ylim([0 200]);
subplot(2,2,3); plot(revxdata,revydata,'ro');
        title('Reverse Data');
        xlabel('Object Distance (cm)');
        ylabel('Image Distance (cm)');
```

```
        hold;
        plot(revsi,revso,'b');
        ylim([0 200]);

%Generation of new dsi/dso data

fwddsidso=(f(1).*f(4)-f(2).*f(3))./(f(3).*fwdso-f(1)).^2;
revdsidso=(r(1).*r(4)-r(2).*r(3))./(r(3).*revso-r(1)).^2;

%This portion of the program will utilize the data
%generated earlier to calculate the matrix elements
%of the complex lens system

%Use a's for forward data
a0=[1 1];
[a resnorm]=lsqcurvefit(@thindsidso2,a0,fwdso,fwddsidso)

%Use b's for reverse data
b0=[1 1];
[b resnorm]=lsqcurvefit(@thindsidso2,b0,revso,revdsidso)

%Calculate Lens Matrix Elements
mc=-1/((b(1)+a(1))/2);
md=mc*(-((a(1)+b(1))/2)-a(2));
ma=1-mc*b(2);
mb=(ma*md-1)/mc;

lensmatrix=[ma mb;mc md]

mp=md/mc;
mq=-ma/mc;

fwdfocallength=abs(mq)
revfocallength=abs(mp)

xdatum=0:0.1:90;
fwdydatum=(-(a(1).^2)./(xdatum-a(2)-a(1)).^2);
revydatum=(-(b(1).^2)./(xdatum-b(2)-b(1)).^2);
subplot(2,2,2); plot(xdatum,fwdydatum);
        ylim([-50,0]);
        title('Forward Data (Asymptote is reverse focal length)');
        xlabel('Object Distance (cm)');
        ylabel('dsi/dso');
        hold;
        plot(fwdso,fwddsidso,'ro');
        xlim([0,150]);
subplot(2,2,4); plot(xdatum,revydatum);
        ylim([-50,0]);
        title('Reverse Data (Asymptote is forward focal length)');
        xlabel('Object Distance (cm)');
        ylabel('dsi/dso');
        hold;
        plot(revso,revdsidso,'ro');
        xlim([0,150]);
```

```
%Calculation of matrix elements for the
%Camera Objective from data collected using
%a 10 nm bandpass filter at 334 nm

clear all

%This portion of the program will load
%the image and object distance measurements
%taken in the lab, fit them to a general
%hyperbolic function, and use that function
%to generate another set of data for further
%analysis

%Import the initial data

load Lens1_334nmdata.dat;

%Create vectors for analysis with the curve
%fitting function
fwdxdata =[[1 0 0 0]*Lens1_334nmdata'];
fwdydata =[[0 1 0 0]*Lens1_334nmdata'];
revxdata =[[0 0 1 0]*Lens1_334nmdata'];
revydata =[[0 0 0 1]*Lens1_334nmdata'];

options=optimset('MaxFunEvals',1e30,'maxiter',5000);

%Use f's for initial curve fit of forward data
f0=[1 1 1 1];
[f resnorm]=lsqcurvefit(@GenHyperbola,f0,fwdxdata,fwdydata);

%Use r's for initial curve fit of reverse data
r0=[1 1 1 1];
[r resnorm]=lsqcurvefit(@GenHyperbola,r0,revxdata,revydata);

%Generation of new image and object distance data

fwdsi=60:0.1:150;
fwdso=((f(1).*fwdsi+f(2))./(f(3).*fwdsi+f(4)));

revsi=60:0.1:150;
revso=((r(1).*revsi+r(2))./(r(3).*revsi+r(4)));

%Plot results for this section

subplot(2,2,1); plot(fwdxdata,fwdydata,'ro');
        title('Forward Data');
        xlabel('Object Distance (cm)');
        ylabel('Image Distance (cm)');
        hold;
        plot(fwdsi,fwdso,'b');
        ylim([0 200]);
subplot(2,2,3); plot(revxdata,revydata,'ro');
        title('Reverse Data');
        xlabel('Object Distance (cm)');
        ylabel('Image Distance (cm)');
```

```
        hold;
        plot(revsi,revso,'b');
        ylim([0 200]);

%Generation of new dsi/dso data

fwddsidso=(f(1).*f(4)-f(2).*f(3))./(f(3).*fwdso-f(1)).^2;
revdsidso=(r(1).*r(4)-r(2).*r(3))./(r(3).*revso-r(1)).^2;

%This portion of the program will utilize the data
%generated earlier to calculate the matrix elements
%of the complex lens system

%Use a's for forward data
a0=[1 1];
[a resnorm]=lsqcurvefit(@thindsidso2,a0,fwdso,fwddsidso)

%Use b's for reverse data
b0=[1 1];
[b resnorm]=lsqcurvefit(@thindsidso2,b0,revso,revdsidso)

%Calculate Lens Matrix Elements
mc=-1/((b(1)+a(1))/2);
md=mc*(-((a(1)+b(1))/2)-a(2));
ma=1-mc*b(2);
mb=(ma*md-1)/mc;

lensmatrix=[ma mb;mc md]

mp=md/mc;
mq=-ma/mc;

fwdfocallength=abs(mq)
revfocallength=abs(mp)

xdatum=0:0.1:90;
fwdydatum=(-(a(1).^2)./(xdatum-a(2)-a(1)).^2);
revydatum=(-(b(1).^2)./(xdatum-b(2)-b(1)).^2);
subplot(2,2,2); plot(xdatum,fwdydatum);
        ylim([-50,0]);
        title('Forward Data (Asymptote is reverse focal length)');
        xlabel('Object Distance (cm)');
        ylabel('dsi/dso');
        hold;
        plot(fwdso,fwddsidso,'ro');
        xlim([0,150]);
subplot(2,2,4); plot(xdatum,revydatum);
        ylim([-50,0]);
        title('Reverse Data (Asymptote is forward focal length)');
        xlabel('Object Distance (cm)');
        ylabel('dsi/dso');
        hold;
        plot(revso,revdsidso,'ro');
        xlim([0,150]);
```

```
%Calculation of matrix elements for the
%Camera Objective from data collected using
%a 10 nm bandpass filter at 370 nm

clear all

%This portion of the program will load
%the image and object distance measurements
%taken in the lab, fit them to a general
%hyperbolic function, and use that function
%to generate another set of data for further
%analysis

%Import the initial data

load Lens1_370nmdata.dat;

%Create vectors for analysis with the curve
%fitting function
fwdxdata =[[1 0 0 0]*Lens1_370nmdata'];
fwdydata =[[0 1 0 0]*Lens1_370nmdata'];
revxdata =[[0 0 1 0]*Lens1_370nmdata'];
revydata =[[0 0 0 1]*Lens1_370nmdata'];

options=optimset('MaxFunEvals',1e30,'maxiter',5000);

%Use f's for initial curve fit of forward data
f0=[1 1 1 1];
[f resnorm]=lsqcurvefit(@GenHyperbola,f0,fwdxdata,fwdydata);

%Use r's for initial curve fit of reverse data
r0=[1 1 1 1];
[r resnorm]=lsqcurvefit(@GenHyperbola,r0,revxdata,revydata);

%Generation of new image and object distance data

fwdsi=60:0.1:150;
fwdso=((f(1).*fwdsi+f(2))./(f(3).*fwdsi+f(4)));

revsi=60:0.1:150;
revso=((r(1).*revsi+r(2))./(r(3).*revsi+r(4)));

%Plot results for this section

subplot(2,2,1); plot(fwdxdata,fwdydata,'ro');
        title('Forward Data');
        xlabel('Object Distance (cm)');
        ylabel('Image Distance (cm)');
        hold;
        plot(fwdsi,fwdso,'b');
        ylim([0 200]);
subplot(2,2,3); plot(revxdata,revydata,'ro');
        title('Reverse Data');
        xlabel('Object Distance (cm)');
        ylabel('Image Distance (cm)');
```

```
        hold;
        plot(revsi,revso,'b');
        ylim([0 200]);

%Generation of new dsi/dso data

fwddsidso=(f(1).*f(4)-f(2).*f(3))./(f(3).*fwdso-f(1)).^2;
revdsidso=(r(1).*r(4)-r(2).*r(3))./(r(3).*revso-r(1)).^2;

%This portion of the program will utilize the data
%generated earlier to calculate the matrix elements
%of the complex lens system

%Use a's for forward data
a0=[1 1];
[a resnorm]=lsqcurvefit(@thindsidso2,a0,fwdso,fwddsidso)

%Use b's for reverse data
b0=[1 1];
[b resnorm]=lsqcurvefit(@thindsidso2,b0,revso,revdsidso)

%Calculate Lens Matrix Elements
mc=-1/((b(1)+a(1))/2);
md=mc*(-((a(1)+b(1))/2)-a(2));
ma=1-mc*b(2);
mb=(ma*md-1)/mc;

lensmatrix=[ma mb;mc md]

mp=md/mc;
mq=-ma/mc;

fwdfocallength=abs(mq)
revfocallength=abs(mp)

xdatum=0:0.1:90;
fwdydatum=(-(a(1).^2)./(xdatum-a(2)-a(1)).^2);
revydatum=(-(b(1).^2)./(xdatum-b(2)-b(1)).^2);
subplot(2,2,2); plot(xdatum,fwdydatum);
        ylim([-50,0]);
        title('Forward Data (Asymptote is reverse focal length)');
        xlabel('Object Distance (cm)');
        ylabel('dsi/dso');
        hold;
        plot(fwdso,fwddsidso,'ro');
        xlim([0,150]);
subplot(2,2,4); plot(xdatum,revydatum);
        ylim([-50,0]);
        title('Reverse Data (Asymptote is forward focal length)');
        xlabel('Object Distance (cm)');
        ylabel('dsi/dso');
        hold;
        plot(revso,revdsidso,'ro');
        xlim([0,150]);
```

%General Hyperbolic Function

```
function f=GenHyperbola(r,xdata)

f=((r(1).*xdata+r(2))./(r(3).*xdata+r(4)));
```

%Function relating dsi/dso and focal length
%for a theoretical thin lens

```
function f=thindsidso2(x,xdata)

f=(-(x(1).^2)./(xdata-x(2)-x(1)).^2);
```

THIS PAGE INTENTIONALLY LEFT BLANK

LIST OF REFERENCES

1. Marino, S. A., *Operation and Calibration of the NPS Ultraviolet Imaging Spectrometer (NUVIS) in the Detection of Sulfur Dioxide Plumes,* Master's Thesis, Naval Postgraduate School, Monterey, California, December 1999.

2. Gerrard, A. and Burch, J. M., *Introduction To Matrix Methods In Optics,* Dover Publications Inc., 1975.

3. Pedrotti, F. L. and Pedrotti, L. S., *Introduction to Optics,* Second Edition, Prentice Hall, 1993.

THIS PAGE INTENTIONALLY LEFT BLANK

INITIAL DISTRIBUTION LIST

1. Defense Technical Information Center
   Ft. Belvoir, Virginia

2. Dudley Knox Library
   Naval Postgraduate School
   Monterey, California 93943-5101

3. David S. Davis
   Naval Postgraduate School
   Monterey, California

4. Richard M. Harkins
   Naval Postgraduate School
   Monterey, California

5. Richard C. Olson
   Naval Postgraduate School
   Monterey, California

6. William Maier
   Naval Postgraduate School
   Monterey, California